

Augmentation of Anticancer Drug Efficacy in Murine Hepatocellular Carcinoma Cells by a Peripherally Acting Competitive *N*-Methyl-D-aspartate (NMDA) Receptor Antagonist

Mikko Gynther,^{*,†,‡} Ilaria Proietti Silvestri,^{†,‡} Jacob C. Hansen,[†] Kasper B. Hansen,^{§,‡} Tarja Malm,^{||} Yevheniia Ishchenko,^{||} Younes Larsen,[†] Liwei Han,[†] Silke Kayser,[†] Seppo Auriola,[‡] Aleksanteri Petsalo,[‡] Birgitte Nielsen,[†] Darryl S. Pickering,^{†,||} and Lennart Bunch^{*,†,||}

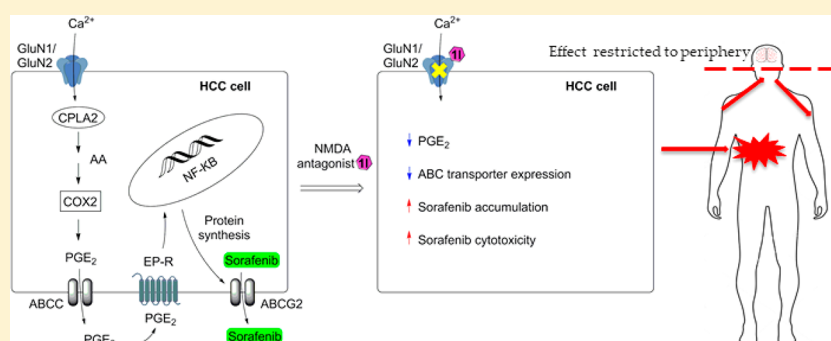
[†]Department of Drug Design and Pharmacology, Faculty of Health and Medical Sciences, University of Copenhagen, Copenhagen 2100, Denmark

[‡]School of Pharmacy, Faculty of Health Sciences, University of Eastern Finland, 70211 Kuopio, Finland

[§]Department of Biomedical and Pharmaceutical Sciences and Center for Biomolecular Structure and Dynamics, University of Montana, Missoula, Montana 59812, United States

^{||}Department of Neurobiology, A.I. Virtanen Institute for Molecular Sciences, University of Eastern Finland, 70211 Kuopio, Finland

Supporting Information



ABSTRACT: The most common solid tumors show intrinsic multidrug resistance (MDR) or inevitably acquire such when treated with anticancer drugs. In this work, we describe the discovery of a peripherally restricted, potent, competitive NMDA receptor antagonist **II** by a structure–activity study of the broad-acting ionotropic glutamate receptor antagonist **Ia**. Subsequently, we demonstrate that **II** augments the cytotoxic action of sorafenib in murine hepatocellular carcinoma cells. The underlying biological mechanism was shown to be interference with the lipid signaling pathway, leading to reduced expression of MDR transporters and thereby an increased accumulation of sorafenib in the cancer cells. Interference with lipid signaling pathways by NMDA receptor inhibition is a novel and promising strategy for reversing transporter-mediated chemoresistance in cancer cells.

INTRODUCTION

Over time, solid tumors inevitably acquire resistance against anticancer therapy, a phenomenon known as multidrug resistance (MDR).¹ However, more devastating are cancers, such as hepatocellular carcinoma (HCC), that exert intrinsic drug-resistance.² A key mechanism underlying MDR is increased expression of ATP-binding cassette (ABC) transporters, which expel a broad range of chemotherapeutic agents from the cancer cells.³ According to current knowledge, the principal ABC transporters responsible for chemoresistance in humans are ATP-binding cassette subfamily B member 1 (ABCB1, Pgp), ATP-binding cassette subfamily G member 2 (ABCG2, BCRP), and ATP-binding cassette subfamily C (ABCC, MRP).^{4–7} In regard to HCC, these transporters are responsible for expelling the first line HCC drug sorafenib from

the cancer cells.^{8–10} The general strategy to reverse MDR has been to coadminister ABC transporter inhibitors with anticancer drugs.¹¹ However, several complications limit the use of ABC transporter inhibitors, among them the fact that ABC transporters are also present in normal cells, leading to undesired drug accumulation.¹¹ Thus, a change of strategy is needed to overcome ABC transporter-mediated chemoresistance.

One such strategy is to downregulate efflux transporter expression by alternating the cell lipid signaling pathway by blocking the *N*-methyl-D-aspartate (NMDA) receptors.¹² NMDA receptors are a subclass of ionotropic glutamate

Received: November 3, 2017

receptors (iGluRs), which also comprises the α -amino-3-hydroxy-5-methyl-4-isoxazolepropionic acid (AMPA) receptors and the kainic acid (KA) receptors.¹³ NMDA receptor activation increases calcium entry, which activates cytoplasmic phospholipase A2 (cPLA2), leading to increased production of arachidonic acid (Figure 1).^{14,15} This fatty acid is further

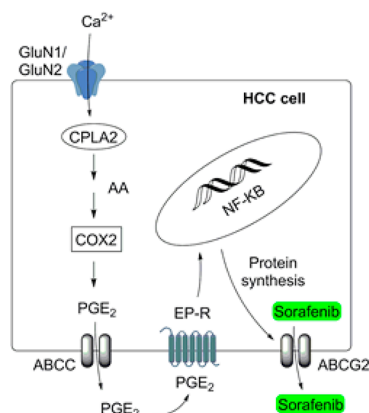


Figure 1. Activation of the lipid signaling pathway by GluN1/GluN2A receptor and the creation of transporter mediated drug resistance. NMDA binding to the GluN1/GluN2A receptor allows the influx of Ca^{2+} into the cell, which leads to cPLA2 activation and the release of arachidonic acid (AA) from phospholipids. Arachidonic acid is metabolized to PGE_2 , which is transported by ABC transporters out of the cell allowing the PGE_2 binding to EP-R. The EP-R activation leads to nuclear translocation of NF- κB followed by ABCG2 protein transcription and MDR.^{12,14–17}

converted to the proinflammatory lipid, prostaglandin-E2 (PGE_2), and actively transported into the extracellular space by ABC transporters, where it binds to the prostaglandin E receptors (EP-Rs), leading to NF- κB activation and creating a positive feedback loop creating an inflammation microenvironment.^{12,14} It has been shown that NF- κB activation results in increased cancer cell survival and proliferation as well as chemoresistance due to elevated ABC transporter and CYP enzyme expression.^{12,16,17}

NMDA receptors are overexpressed on the cell membrane of many types of cancer cells, including HCC.¹⁸ The non-competitive NMDA receptor antagonist MK-801 (Figure 2) has previously been shown to augment the antiproliferative efficacy of antiestrogens in melanoma cells¹⁹ and suppress the growth of HCC cells.²⁰ The antiproliferative effect of MK-801 in HCC cells was shown to be mediated through the FOXO/XTNIP pathway, which is not connected to pro-inflammatory lipid signaling. Moreover, the impact of NMDA receptor antagonists on transporter expression, anticancer drug accumulation, and efficacy in cancers has not been studied. Most importantly, a competitive NMDA receptor antagonist for use as an augmentative drug for the treatment of peripheral solid tumors must not be capable of crossing the blood–brain barrier (BBB), as this would otherwise lead to severe adverse effects, including psychosis.²¹

In the present study, we report the design and synthesis of the novel peripherally acting potent NMDA receptor antagonist **11**. We describe the ability of **11** to modulate the cPLA2 activation-dependent lipid signaling pathway, downregulate ABC transporter expression, and thereby augment the cytotoxic efficacy of the anticancer drug sorafenib in murine HCC cells.

RESULTS AND DISCUSSION

The two commonly studied competitive NMDA receptor antagonists that do not penetrate the BBB are D-AP5 and (*R*)-CPP (Figure 2). Both are amino acid analogs and highly polar with calculated partition coefficient values in octanol/water ($\text{cLogP}(\text{o/w})$) well below zero (-1.7 and -2.2 , respectively). In comparison with recommended $\text{cLogP}(\text{o/w})$ values of -0.4 to 5.6 ²² for oral bioavailability, we believed that these NMDA receptor antagonists were not attractive candidates for this study.

We therefore turned to the previously reported nonselective iGluR antagonist **1a** (Figure 2 and Table 1).²³ The facts that **1a** does not penetrate the BBB in mouse in situ brain perfusion and that its $\text{cLogP}(\text{o/w})$ value is calculated at 1.3 make it an attractive starting point for the purpose of developing an orally available, peripherally restricted, competitive NMDA receptor antagonist.²²

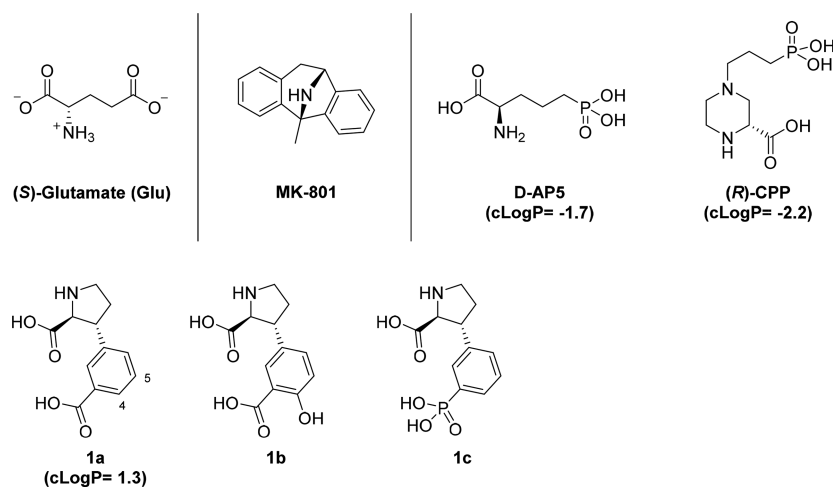
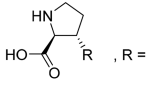
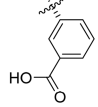
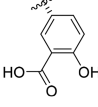
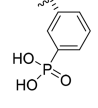
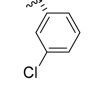
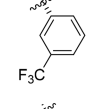
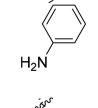
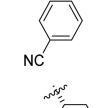
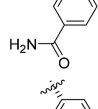
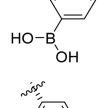
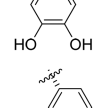
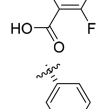
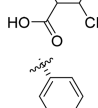
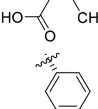
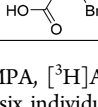


Figure 2. Chemical structures of Glu, selective uncompetitive NMDA receptor antagonist MK-801, selective competitive NMDA receptor antagonists D-AP5, (*R*)-CPP, and competitive iGluR antagonist **1a**, including published analogs **1b,c** with relevance to the SAR study reported herein.

Table 1. Binding Affinities of 1a–n at Native AMPA, KA, and NMDA Receptors (Rat Synaptosomes) and Cloned Homomeric Receptors GluK1–3^a

Cmpd No		AMPA IC ₅₀ (μM)	KA IC ₅₀ (μM)	NMDA K _i (μM)	GluK1 K _i (μM)	GluK2 K _i (μM)	GluK3 K _i (μM)
1a ²³		51	22	6.0	4.3	>100	8.1
1b ²⁴		2.0	1.4	1.0	4.8	10–100	0.87
1c ²⁴		>100	>100	>100	126	>1000	78
1d		>100	>100	>100	>100	>100	>100
1e		>100	>100	>100	>100	>100	>100
1f		>100	>100	>100	--	--	--
1g		>100	>100	>100	>1000	>1000	>1000
1h		>100	>100	>100	>100	>100	>100
1i		>100	>100	>100	>1000	>1000	>100
1j		>100	>100	35 [4.46 ± 0.04]	--	--	--
1k		>100	59 [4.23 ± 0.05]	4.6 [5.34 ± 0.04]	12 ± 0.5	>100	11 ± 0.97
1l		>100	>100	0.63 [6.22 ± 0.10]	154 ± 13	>100	131 ± 13
1m		>100	>100	17 [4.78 ± 0.04]	>100	>100	>100
1n		>100	>100	0.62 [6.22 ± 0.07]	>100	>100	>100

^a--: not tested. Radio ligands: AMPA, [³H]AMPA; KA, [³H]KA; NMDA, [³H]CGP-39653; GluK1, [³H]SYM2081; GluK2 and GluK3, [³H]KA. Data are mean values of three to six individual experiments performed in triplicate. For AMPA and KA: pIC₅₀ values with SEM in brackets. For NMDA: pK_i values with SEM in brackets.

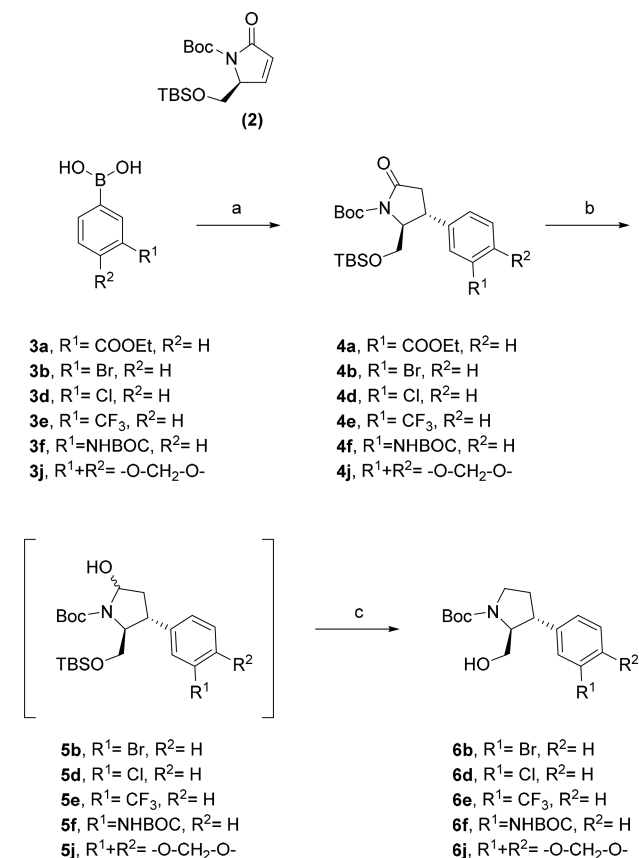
We have previously reported the first structure–activity relationship (SAR) study on **1a**, which disclosed the 4-position on the aryl ring as a hotspot for induction of KA receptor subtype selectivity (compound **1b**, Figure 2 and Table 1). Also, it was seen that simple lipophilic substituents in the 5-position did not lead to any significant improvement in receptor selectivity or higher affinity (structures not shown).²⁴ The 3-carboxylic acid functionality was displaced with a phosphonic acid group, compound **1c** (Figure 2), which led to a significant reduction in binding affinity at the iGluRs (Table 1).²⁴

With this SAR information in hand, we set out to investigate two strategies with the aim of improving iGluR class selectivity. First, we wanted to substitute the 3-carboxylic acid functionality with different functional groups (analogs **1d–j**). While it is well-accepted that the γ -carboxylate functionality in Glu is mandatory for agonist activity at the iGluRs,¹³ it remains an open question if nonionizable distal functional groups can stabilize the NMDA receptor in its open antagonist state. Based on synthetic tractability, the following seven analogs were thus designed: 3-chloro (**1d**), 3-trifluoromethyl (**1e**), 3-amino (**1f**), 3-cyano (**1g**), 3-carbamido (**1h**), 3-boronic acid (**1i**), and 3,4-dihydroxy (**1j**). The synthesis of **1d–j** was carried out by a stereoselective rhodium(I)-catalyzed addition of an arylboronic acid to protected enone **2**²⁴ as the key step (Scheme 1).²⁵ Hereby, the 2,3-*trans* stereochemistry on the proline ring was set, and subsequent functional group transformations in accordance with earlier reported strategies (**1d–f**, Scheme 2; **1g,h**, Scheme 3; **1i**, Scheme 4; **1j**, Scheme 5) gave the free amino acids **1d–j** ready for pharmacological evaluation.^{23,24}

The second series of analogs, compounds **1k–n**, aimed to further explore the impact of substituents in the 4-position of the aryl ring. We have previously shown that introduction of a 4-hydroxy group (analog **1b**) resulted in generally enhanced affinity for iGluRs with a 10-fold improvement for the GluK3 subunit (Table 1).²⁴ Given the hydrogen bond donor and acceptor abilities of the 4-hydroxyl group, three new analogs were designed to address the influence of these features: 4-fluoro (**1k**), 4-chloro (**1l**), and 4-methyl (**1m**). For **1k** and **1l**, the syntheses were based on the stereoselective conjugate addition of an in situ formed aryl cuprate to enone **2**,^{24,26} whereas for **1m** the afore-applied protocol of rhodium(I)-catalyzed addition of a boronic ester to enone **2** was used (Scheme 6). Subsequent functional group transformations to obtain the free amino acids **1k–m** followed the strategy for comparable analogs previously reported by us.^{23,24}

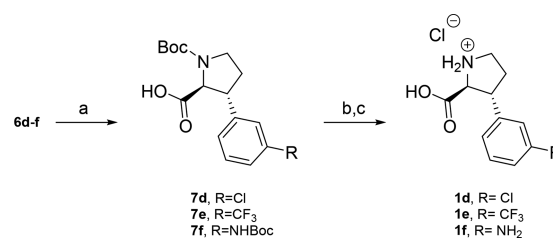
Binding affinities of the synthesized amino acids **1d–n** were determined at native AMPA, KA, and NMDA receptors (rat synaptosomes) and cloned rat homomeric subtypes GluK1–3, and results are summarized in Table 1. The 3-chloro, 3-trifluoromethyl, 3-amino, and 3-cyano analogs, **1d–g**, respectively, all showed insignificant binding affinity for any of the iGluRs (IC_{50} or $K_i > 100 \mu\text{M}$). Furthermore, 3-carbamido analog **1h** and 3-boronic acid analog **1i** did not display notable binding affinities for native iGluRs nor for homomeric GluK1–3 receptors (IC_{50} or $K_i > 100 \mu\text{M}$). Finally, the 3,4-dihydroxy analog **1j** was a weak binder at the NMDA receptors ($K_i = 35 \mu\text{M}$). While these results were all together disappointing, the affinity profiles for the 4-substituted analogs **1k–m** were in contrast exciting. In comparison with the 4-hydroxy analog **1b**, the 4-fluoro analog **1k** displayed the first

Scheme 1. Synthesis of Key Alcohol Intermediates **6b,d–f,j** via Rhodium(I)-Catalyzed 1,4 Addition of Respective Boronic Acids **3a,b,d–f,j** to Enone **2**^a



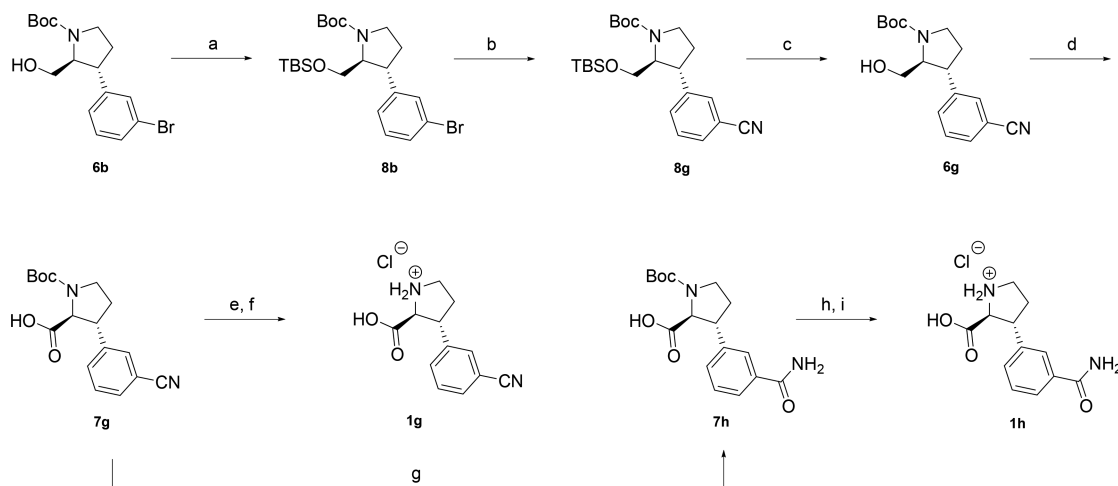
^aReagents and conditions: (a) [Rh(cod)Cl]₂, H₂O, Cs₂CO₃, enone **2**, THF or dioxane, rt (52–67%); (b) LiBEt₃H, THF, -78 °C; (c) HSiEt₃, BF₃·Et₂O, DCM, -78 °C (31–78%).

Scheme 2. Synthesis of **1d–f** from Alcohols **6d–f**, Respectively^a

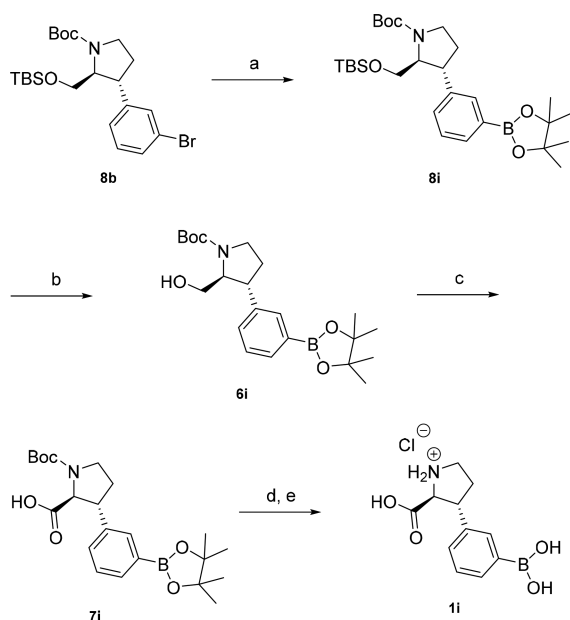


^aReagents and conditions: (a) RuCl₃·xH₂O, NaIO₄, EtOAc/MeCN/H₂O (49–86%); (b) TFA, DCM, rt; (c) 1 M HCl (12–78%).

steps toward selectivity for the NMDA receptors by showing a lower affinity for native AMPA and KA receptors as well as for homomeric GluK1–3 receptors. This trend was boosted significantly for 4-chloro analog **1l**, which proved to be selective for native NMDA receptors with submicromolar binding affinity ($K_i = 0.63 \mu\text{M}$). Also for 4-bromo analog **1n**,²⁷ full selectivity for NMDA receptors was observed with binding affinity similar to **1l** ($K_i = 0.62 \mu\text{M}$). In contrast to this

Scheme 3. Synthesis of 3-Cyano Analog 1g from Alcohol 6b and 3-Carbamido Analog 1h from 7g^a

^aReagents and conditions: (a) TBSCl, imidazole, DMF, rt (73%, three steps from 4b); (b) Zn(CN)₂, Pd₂(dba)₃, dppf, DMA, 120 °C; (c) TBAF, THF, rt (71%, two steps); (d) RuCl₃·xH₂O, NaIO₄, EtOAc/MeCN/H₂O (76%); (e) TFA, DCM, rt; (f) 1 M HCl (81%, two steps); (g) 30% H₂O₂, K₂CO₃, EtOH/H₂O, rt (66%); (h) TFA, DCM, rt; (i) 1 M HCl (59% after three steps).

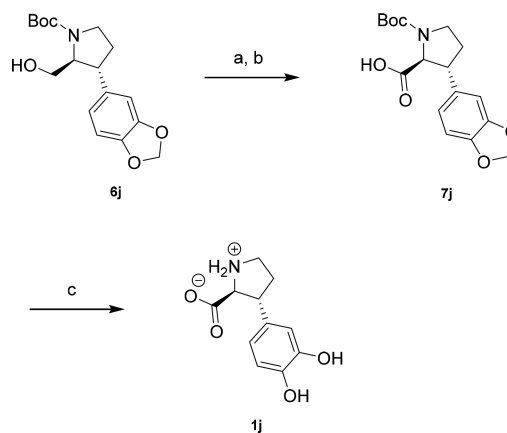
Scheme 4. Synthesis of 3-Boronic Acid Analog 1i, Starting from Bromine 8b^a

^aReagents and conditions: (a) KOAc, Pd₂(dba)₃, dppf, DMF (61%); (b) TBAF, THF, rt (60%); (c) RuCl₃·xH₂O, NaIO₄, EtOAc/MeCN/H₂O (65%); (d) TFA, DCM, rt; (e) 1 M HCl (40%, two steps).

important finding, the binding affinity for native NMDA receptors dropped 30-fold for the 4-methyl analog 1m.

The cLogP(o/w) values of 11 and 1n were calculated at 1.9 and 2.1, respectively, placing both analogs in the recommended cLogP interval of -0.4 to 5.6 for good bioavailability.²² Given that an aryl bromide is a less attractive functional group in compounds for biological administration compared to an aryl chloride, compound 11 was selected for further functional studies at NMDA receptors.

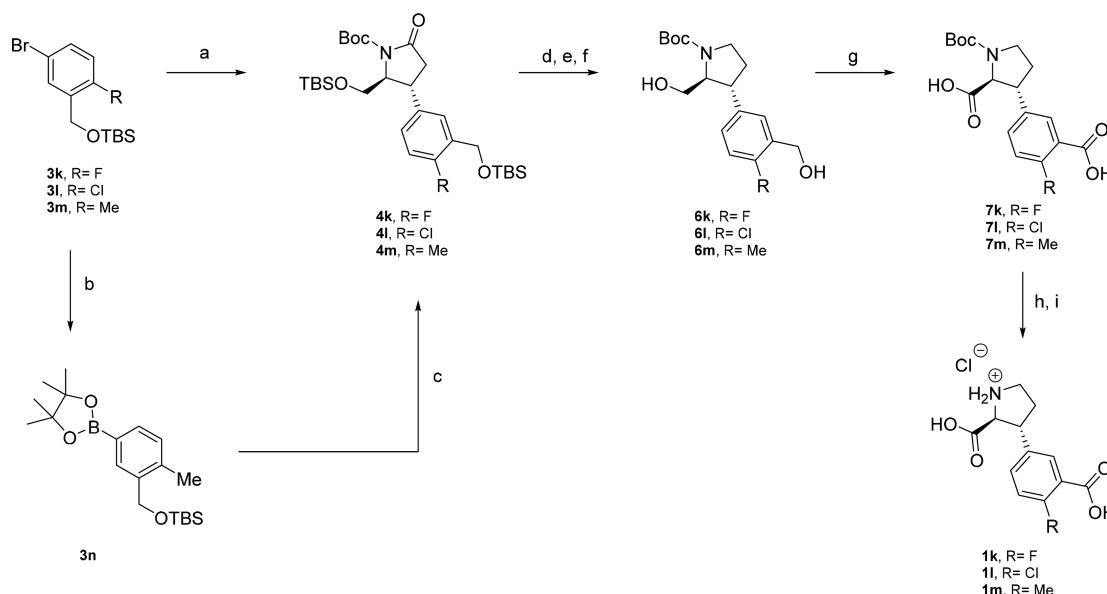
Functional Characterization of 11 at NMDA Receptor Subtypes. Compound 11 was next evaluated in a functional assay at the four NMDA receptor subtypes, GluN1/GluN2A-D (Figure 3 and Table 2). At all four subtypes, 11 was found to be

Scheme 5. Synthesis of 1j from Alcohol 6j^a

^aReagents and conditions: (a) IBX, DMSO, rt; (b) NaClO₂, NaH₂PO₄, 2-methyl-2-butene, *tert*-BuOH/H₂O, rt (66%, two steps); (c) BBr₃, DCM (8% after recrystallization from MeOH).

a competitive antagonist with K_i values of 4.7, 10, 24, and 41 μM, respectively, and the selectivity profile of 11 was similar to D-AP5 (K_i values of 0.39, 2.8, 5.9, and 21, respectively²⁸).

Pharmacokinetics of Compound 11 in Mice. With the attractive pharmacological profile of 11 in hand, we turned to determine its pharmacokinetics and brain permeation. The pharmacokinetic analysis was performed by 10 mg/kg i.p. injection at five time points between 10 and 240 min. The apparent pharmacokinetic parameters, area under the concentration–time curve from time zero to 240 min (AUC_{0–240 min}), the maximum concentration after dosing (C_{max}), time to reach C_{max} (t_{max}), and elimination half-life (t_{1/2β}) in plasma, liver, and brain, calculated from the *in vivo* data are presented in Table 3. The compound was absorbed from the injection site, and concentrations above the K_i value were detected from both plasma and liver. The K_p liver/plasma value was 0.19. Importantly, compound 11 did not exhibit BBB permeation and was detected only at 30 and 60 min time points with concentrations of 0.3 and 0.1 nmol/g, respectively. We confirmed the poor BBB permeation using an *in situ* mouse brain perfusion technique.

Scheme 6. Synthesis of 1k–l via Copper(I)-Catalyzed Addition to Enone 2 and Im via Rhodium(I)-Catalyzed Addition to Enone 2^a

^aReagents and conditions: (a) for 3k,l, *n*-BuLi, CuCN, then enone 2, Et₂O, -78 to -42 °C (46% and 73%); (b) for 3m, (Bpin)₂, KOAc, (PPh₃)₂PdCl₂ (quant); (c) [Rh(cod)Cl]₂, H₂O, Cs₂CO₃, enone 2, rt (41%); (d) for 4k,l, LiBEt₃H, THF, -78 °C, then HSiEt₃, BF₃·Et₂O, DCM, -78 °C; (e) for 4m, BH₃·SMe₂, THF, reflux; (f) TBAF, THF, rt. (20% and 49%); (g) RuCl₃·xH₂O, NaIO₄, EtOAc/MeCN/H₂O (20–97%); (h) TFA, DCM, rt; (i) 1 M HCl (56–60%).

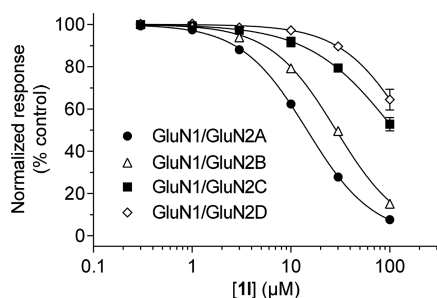


Figure 3. Concentration–inhibition data for **1l** at recombinant NMDA receptor subtypes GluN1/GluN2A–D. Responses were measured using two-electrode voltage-clamp electrophysiology and were activated by coapplication of 100 μM glycine and Glu to *Xenopus* oocytes expressing recombinant NMDA receptors subtypes. Ten micromolar Glu was used for GluN1/GluN2A, 3 μM Glu for GluN1/GluN2B and GluN1/GluN2C, and 1 μM Glu for GluN1/GluN2D receptors. Data are mean ± SD (error bars are mostly contained within the symbols). See Table 2 for IC₅₀ and estimated K_i values.

The brain concentration of compound **1l** following perfusion with 100 μM compound was below the detection limit of our analytical method (5 pmol/g). Moreover, there were no observable changes in the behavior of the mice after **1l** injection. This supports our findings from the *in vivo* pharmacokinetic experiments that **1l** is a fully peripherally restricted NMDA receptor antagonist suitable for affecting peripheral tumors. In addition to hepatocellular carcinoma, NMDA receptor expression has been reported to be elevated in colon, prostate, and breast cancers compared to healthy tissues.¹⁸ Moreover, the lack of pharmacological effect in the CNS provides the possibility to utilize the compound as a research tool for investigating the role of peripheral NMDA receptors in other diseases and/or conditions such as chronic pain.

Table 2. Inhibition of Recombinant NMDA Receptor Subtypes by **1l**^a

	IC ₅₀ (μM)	n _H	estimated K _i (μM)	N
GluN1/GluN2A	15 ± 1	1.3	4.7 ± 0.1	7
GluN1/GluN2B	29 ± 1	1.3	10 ± 1	5
GluN1/GluN2C	110 ± 8	1.0	24 ± 2	4
GluN1/GluN2D	170 ± 10	1.3	41 ± 3	7

^aIC₅₀ values for inhibition of current responses activated by coapplication of 100 μM glycine and Glu to *Xenopus* oocytes expressing recombinant rat GluN1/GluN2A–D NMDA receptors. Responses were activated by Glu concentrations 2- to 3-fold higher than the EC₅₀ at the respective NMDA receptor subtypes; 10 μM Glu was used for GluN1/GluN2A, 3 μM Glu for GluN1/GluN2B and GluN1/GluN2C, and 1 μM Glu for GluN1/GluN2D receptors. K_i values were estimated using the Cheng–Prusoff relationship²⁹ and previously determined Glu EC₅₀ values.³⁰ IC₅₀ and K_i values are mean ± SEM, n_H is the Hill slope, and N is the number of oocytes.

Table 3. Pharmacokinetic Parameters of Compound **1l** in Plasma, Liver, and Brain Calculated from *in Vivo* Data after a Single Dose of 10 mg/kg i.p. in Mice

	plasma	liver	brain
AUC _(0–240 min) (nmol/g·min)	3020	575	13
C _{max} (nmol/g)	43.4	8.7	0.3
t _{max} (min)	15	30	30
t _{1/2β} (min)	30	36	ND

Ability of Compound 1l To Inhibit NMDA Receptor Expressed in Murine HCC Cells. With compound **1l** in hand, we proceeded to studies of its *in vitro* efficacy in mice. First, we confirmed the expression of the GluN1 NMDA receptor subunit in the murine HCC cell line by Western immunoblotting (data not shown). In order to assess the function of NMDA receptors in the murine HCC cell culture we used

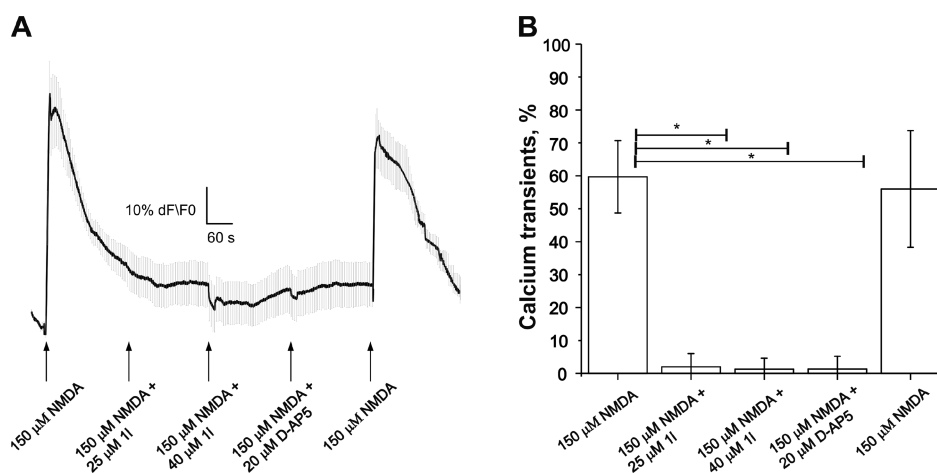


Figure 4. Ca²⁺ transients via NMDA receptors in murine HCC cells. (A) Ca²⁺ transients in HCC cells activated by NMDA applications (15 s) with and without NMDA receptor antagonists (**11** and D-AP5). (B) Histogram showing percentage of induced Ca²⁺ transients in a response to NMDA application and absence of the activation while applied together with **11** at 25 and 41 μM concentration and D-AP5 at 20 μM concentration. Quantitative data were expressed as mean ± SEM (*n* = 5). The statistical significance was assessed with the Student-paired *t* test or Mann–Whitney *U* test for nonparametric data. Statistically significant differences were set at **P* < 0.05.

calcium imaging (Figure 4). To compare the abilities of **11** and D-AP5 to inhibit NMDA receptor activation, we measured the intracellular Ca²⁺ transients induced by 150 μM NMDA alone and in the presence of the compound **11** (25 and 40 μM) or D-AP5 (20 μM). Both compounds were able to inhibit NMDA receptor activation significantly in the murine HCC cells suggesting their ability to antagonize the lipid signaling pathway in cancer cells.

Ability of Compound 11 To Decrease PGE₂ Concentration in Murine HCC Cells. The ability of compound **11** to decrease the extracellular PGE₂ concentration in murine HCC cells was investigated by incubating the cells in 24-well plates for 24 h with 100 μM **11**. In addition, the PGE₂ concentration was measured from HCC cells with lipopolysaccharide (LPS) induced inflammation using the same compound **11** concentration and incubation time (Figure 5). Compound **11** significantly decreased the PGE₂ concentration in both the presence and absence of LPS, confirming that the compound is able to interfere with the synthesis of PGE₂. This inhibition of PGE₂ production will reduce the proinflammatory lipid signaling pathway in HCC cells, which has been suggested to downregulate ABC transporters in cancer cells.^{12,14–16}

Effect of the Compound 11 on Transporter Expression in Mouse HCC Cells. Expression levels of Abcb1, Abcg2, Abcc2, and Abcc4 as well as Slc7a5 and Slc2a1 in HCC cells were determined by selected/multiple reaction monitoring (SRM/MRM) analysis in liquid chromatography–tandem mass spectrometry (LC–MS/MS),³¹ following administration of 10 μM **11** and compared to control. Compound **11** reduced the expression levels of Abcb1 and Abcg2 transporters in the crude membrane fraction by 39% and 34%, respectively (Table 4). Abcc4 protein expression was reduced by 14%, but the reduction was not statistically significant, and Abcc2 protein expression was below the lower limit of quantification. Interestingly, the expression of Slc2a1 and Slc7a5 transporter proteins was decreased by 42% and 24%, respectively. However, the difference in the case of Slc7a5 was not statistically significant. In all, these findings evidence that NMDA receptor antagonism results in downregulation of ABC transporter expression in HCC cells. In addition, the expression of the two investigated nutrient transporters was reduced. In

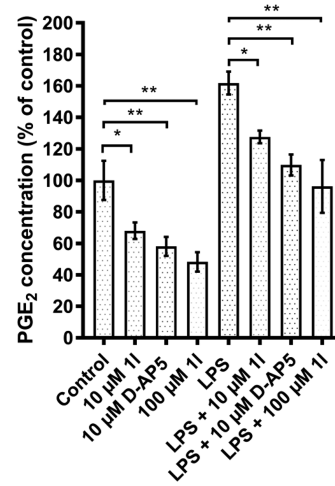


Figure 5. Effect of compound **11** and D-AP5 on PGE₂ levels in HCC cells. Compounds **11** and D-AP5 at 10 μM and compound **11** at 100 μM reduced the concentration of PGE₂ after 24 h incubation to 68 ± 5%, 58 ± 6%, and 48 ± 6%, respectively. The addition of LPS (2.5 μg/mL) increased the PGE₂ concentration to 162 ± 7%, and the addition of compounds **11** and D-AP5 at 10 μM as well as compound **11** at 100 μM prevented the effect of LPS, reducing the PGE₂ concentrations to 127 ± 4%, 110 ± 7%, and 96 ± 17%, respectively. The data is presented as mean ± SEM, *n* = 3. The statistical significance of differences in PGE₂ concentrations between treatments was determined using one-way ANOVA and Tukey's test (**P* < 0.05, ***P* < 0.01).

order to further study the significance of the transporter downregulation, we investigated the cell accumulation of transporter probes and sorafenib.

Ability of NMDA Receptor Antagonist **11** To Alter the Cell Accumulation of Transporter Probes and Sorafenib.

To investigate the ability of compound **11** to reverse ABC transporter mediated MDR and decrease the uptake of essential nutrients in murine HCC cells, we determined the intracellular accumulation of known ABC transporter substrates: Abcb1 probe [³H]-digoxin,³² Abcc1–5 probe fluorescein,³³ Abcb1 and Abcg2 substrate sorafenib (Figure 6) as well as Slc7a5 substrate [¹⁴C]-L-leucine and Slc2a1 substrate [¹⁴C]-D-glucose (Figure

Table 4. ABC Transporter Expression Levels in Mouse HCC Cell Crude Membrane Fraction Measured by SMR/MRM Analysis

	protein expression level (fmol/ μ g of total protein)					
	Abcb1 (Pgp)	Abcg2 (Bcrp)	Abcc2 (Mrp2)	Abcc4 (Mrp4)	Slc2a1 (Glut1)	Slc7a5 (Lat1)
control	0.64 \pm 0.08	1.88 \pm 0.04	<i>a</i>	0.31 \pm 0.04	22.7 \pm 0.84	7.55 \pm 0.28
10 μ M 11	0.39 \pm 0.06 ^{<i>ca</i>}	1.24 \pm 0.13 ^{<i>**</i>}	<i>a</i>	0.27 \pm 0.04	13.2 \pm 0.53 ^{<i>***</i>}	5.72 \pm 1.61

^abelow the lower limit of quantification. The statistical difference between compound **11**-treated cells and the control cells was determined using unpaired two-tailed *t* test (^{*}*P* < 0.05, ^{**}*P* < 0.01, ^{***}*P* < 0.001). Data are presented as mean \pm SEM (*n* = 4).

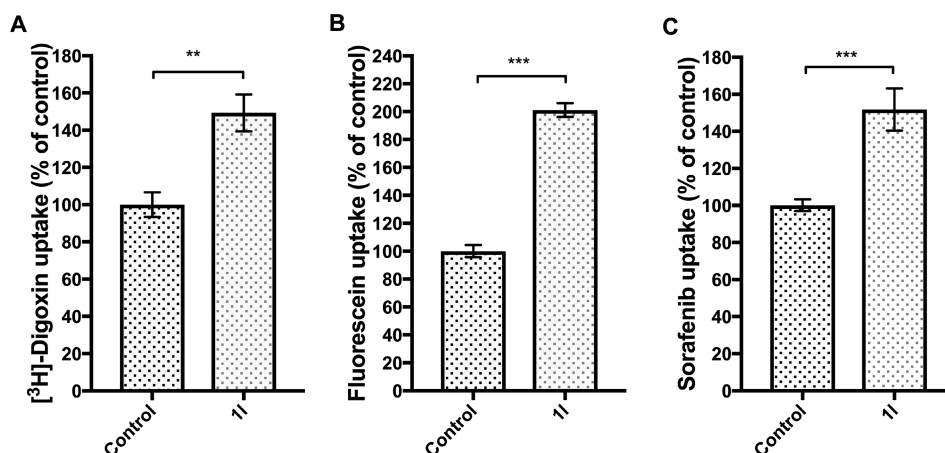


Figure 6. Effect of compound **11** on cell accumulation of efflux probes [³H]-digoxin, fluorescein, and sorafenib. The incubation of the HCC cells with 10 μ M compound **11** increased the cell accumulation of (A) [³H]-digoxin, (B) fluorescein, and (C) sorafenib to 149% \pm 10%, 201% \pm 9%, and 152% \pm 11%, respectively. The analyte concentrations are normalized by the amount of protein in each sample. The statistical difference between compound **11**-treated cell and the control cells was determined using unpaired two-tailed *t* test (^{**}*P* < 0.01, ^{***}*P* < 0.001). Data are presented as mean \pm SEM (*n* = 3).

7).^{8–10} The cells were incubated with or without 10 μ M of compound **11** in the growth medium for 24 h. Accumulation of the efflux probes in the cells was significantly increased after incubating the cells with compound **11**. In addition, the cell uptake of [¹⁴C]-L-leucine was reduced significantly. Therefore, the data provides evidence that the reduced transporter expression levels are significant enough to lead to reduced

transporter activity. The risk of compound **11** to interfere with transporter function was minimized by washing the cells before uptake experiments. Thus, the increased cell accumulation of transporter probes is not likely due to compound **11** acting as a transporter inhibitor, but as a modulator of transporter expression.

Effect of Compound 11 on Sorafenib Cytotoxicity in Mouse HCC Cells. The half maximal inhibitory concentration (IC₅₀) value of sorafenib on HCC cell viability was investigated at 72 h using concentration range from 0.1 to 200 μ M (Figure 8A). The effect of **11** on HCC cell proliferation and the possible potentiating effect on sorafenib cytotoxicity were evaluated by incubating the HCC cells for 72 h at different sorafenib concentrations with and without a 100 μ M concentration of **11** (Figure 8B). Interestingly, **11** significantly augmented the efficacy of sorafenib at 1, 2.5, and 5 μ M concentrations. At 10 μ M sorafenib concentration, NMDA receptor antagonist **11** also augmented sorafenib efficacy, although the effect was less pronounced. On its own the NMDA antagonist **11** was only able to reduce HCC cell proliferation slightly. In addition, D-AP5 had a potentiating effect on sorafenib cytotoxicity at all sorafenib concentrations investigated (Figure 8C). Previously it was shown that at above 100 μ M concentrations a non-competitive NMDA receptor antagonist has antiproliferative effects on HCC cells affecting the FOXO/TXNIP pathway. Therefore, the antiproliferative effect of **11** alone is likely mediated via the same pathway. However, as sorafenib exerts its effect through the RAF/MEK/ERK pathway,³⁴ the potentiating effect of **11** is more likely mediated through the lipid signaling pathway and downregulation of efflux transporter expression.

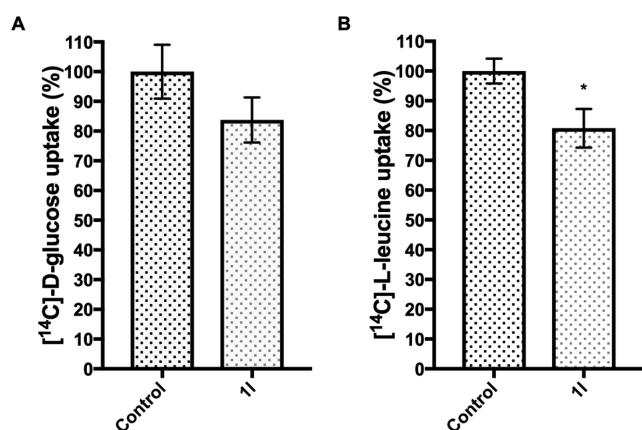


Figure 7. Effect of compound **11** on cell accumulation of Slc2a1 and Slc7a5 transporter substrates [¹⁴C]-D-glucose and [¹⁴C]-L-leucine. The incubation of the HCC cells with 10 μ M compound **11** reduced the cell accumulation of (A) [¹⁴C]-D-glucose and (B) [¹⁴C]-L-leucine to 84% \pm 8% and 81% \pm 6%, respectively. The analyte concentrations are normalized by the amount of protein in each sample. The statistical difference between compound **11**-treated cell and the control cells was determined using unpaired two-tailed *t* test (^{*}*P* < 0.05). Data are presented as mean \pm SEM (*n* = 4).

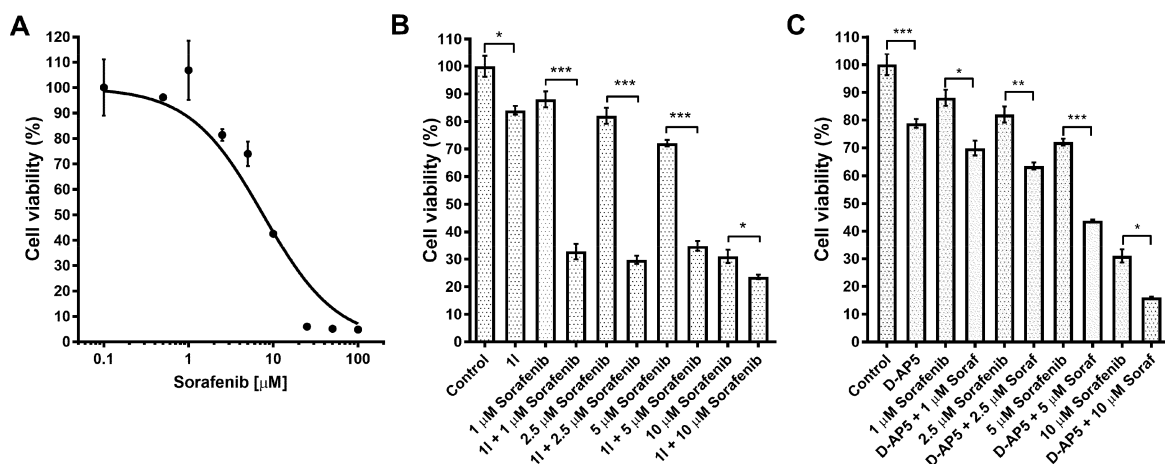


Figure 8. (A) Concentration-dependent antiproliferative efficacy of sorafenib in HCC cells after 72 h. IC_{50} value was $7.4 \pm 1.7 \mu\text{M}$. Ability of compound **11** to potentiate the cytotoxic efficacy of sorafenib in mouse HCC cells. (B) Potentiating effect of compound **11** on sorafenib antiproliferative efficacy in murine HCC cells. Compared to sorafenib effect alone, the cell viability was further reduced in the presence of 100 μM compound **11** from $88 \pm 3\%$ to $33 \pm 3\%$, $82 \pm 3\%$ to $30 \pm 2\%$, $72 \pm 1\%$ to $35 \pm 2\%$, and $31 \pm 2\%$ to $24 \pm 1\%$, at 1, 2.5, 5, and 10 μM sorafenib, respectively. Compound **11** at 100 μM without sorafenib was able to reduce the cell viability to $84 \pm 2\%$. (C) Potentiating effect of D-APS on sorafenib antiproliferative efficacy in murine HCC cells. The cell viability was reduced to $70 \pm 3\%$, $63 \pm 1\%$, $44 \pm 1\%$, and $16 \pm 1\%$, in combination of 100 μM D-APS and 1, 2.5, 5, and 10 μM sorafenib, respectively. D-APS at 100 μM without sorafenib was able to reduce the cell viability to $79 \pm 2\%$. The remaining viability is presented as mean \pm SEM ($n = 3-6$). The statistical difference between groups were determined by one-way ANOVA followed by Tukey's multiple comparison test (* $P < 0.05$, ** $P < 0.01$, *** $P < 0.001$).

CONCLUSION

Starting from the broad-acting iGluR antagonist **1a**, we have developed a potent and selective competitive NMDA receptor antagonist, compound **11**, whose action is restricted to peripheral tissues and which displays good drug-like properties. Application of **11** to murine HCC cells reduced the intracellular concentration of PGE_2 and thereby interfered with the proinflammatory lipid signaling pathway resulting in downregulation of MDR transporters. It was subsequently shown that **11** augments cell accumulation of MDR transporter substrates and that cell accumulation of the HCC anticancer agent and ABC transporter substrate sorafenib was significantly increased leading to augmented cytotoxic efficacy. Another important finding was the significant downregulation of nutrient transporters, which are essential for the rapid growth of cancer cells. In summary, this proof-of-concept study demonstrates that competitive NMDA receptor antagonists represent a novel and promising strategy to reverse MDR in peripheral solid tumors, such as HCC.

EXPERIMENTAL SECTION

Chemistry. All reagents were obtained from commercial suppliers and used without further purification. Dry solvents were obtained differently. THF was distilled over sodium/benzophenone. Et_2O was dried over neatly cut sodium. All solvents were tested for water content using a Carl Fisher apparatus. Water- or air sensitive reactions were conducted in flame-dried glassware under nitrogen with syringe-septum cap technique. Purification by dry column vacuum chromatography (DCVC) was performed with silica gel size 25–40 μm (Merck, Silica gel 60). For TLC, Merck TLC Silica gel F254 plates were used with appropriate spray reagents: KMnO_4 or molybdenum blue. ^1H NMR and ^{13}C NMR spectra were obtained on a Varian Mercury Plus (300 MHz) and a Varian Gemini 2000 instrument (75 MHz), respectively, unless otherwise noted. Dioxane was used as internal reference for NMR spectra run in D_2O . Preparative HPLC was performed using either a Spectraseries UV100 detector with a JASCO 880-PU HPLC pump and an XTerraPrep MS C18 (10 μm , 10 \times 300 mm) column or an Agilent Prep HPLC system, equipped with a 1100 series pump, a 1200 series multiple wavelength detector, and a

Zorbax 300 SB-C18 (21.2 \times 250 mm, 7 μm) column. LC–MS was performed using an Agilent 1200 HPLC system coupled to an Agilent 6400 triple quadrupole mass spectrometer equipped with an electrospray ionization source. A Zorbax Eclipse XDB-C18 (4.6 \times 50 mm) column and gradients of 10% aqueous acetonitrile + 0.05% formic acid (buffer A) and 90% aqueous acetonitrile + 0.046% formic acid (buffer B) were employed. Optical rotation was measured using a PerkinElmer 241 spectrometer, with a Na lamp at 589 nm. Melting points were measured using an automated melting point apparatus, MPA100 OptiMelt (SRS), and are uncorrected. Compounds were dried either under high vacuum or freeze-dried using a Holm and Halby, Heto LyoPro 6000 freeze drier. Compounds for pharmacological characterization were all with a purity of $>95\%$, determined by HPLC (254 nm).

(2S,3R)-2-Carboxy-3-(3-chlorophenyl)pyrrolidin-1-ium Chloride (1d). Acid **7d** (120 mg, 0.37 mmol, 1.0 equiv) was dissolved in a 1:1 mixture of TFA/DCM (7.2 mL). The reaction mixture was allowed to stir for 1 h at rt, then evaporated to dryness under reduced pressure. The solid was dissolved in 1 M HCl (2 mL) and evaporated to dryness (3 \times) to give the crude product, which was recrystallized from MeOH/ CHCl_3 to afford the title compound as white needles (17 mg, 18%). ^1H NMR (CDCl_3) δ (two rotamers) 9.64 (br s, 1H), 7.27–7.22 (m, 3H), 7.15–7.13 (m, 1H), 4.40 (d, $J = 5.5$ Hz, 0.4H), 4.25 (d, $J = 6.5$ Hz, 0.6H), 3.79–3.44 (m, 3H), 2.38–2.28 (m, 1H), 2.06–1.96 (m, 1H), 1.49 (s, 4H), 1.42 (s, 5H). ^{13}C NMR (CDCl_3) δ (two rotamers) 177.6, 175.7, 155.2, 153.7, 142.9, 142.4, 134.6, 130.1, 127.5, 127.4, 127.1, 125.2, 81.2, 80.1, 65.4, 64.9, 49.4, 47.5, 46.1, 45.9, 32.7, 32.2, 28.3, 28.2. MS (m/z) calcd. for $\text{C}_{11}\text{H}_{13}\text{ClNO}_2$ [$\text{M} + \text{H}$] $^+$ 226.1, found 226.1. Mp: decomposition.

(2S,3R)-2-Carboxy-3-(3-(trifluoromethyl)phenyl)pyrrolidin-1-ium Chloride (1e). Compound **7e** (135 mg) was dissolved in a 1:1 mixture TFA/DCM (7.0 mL). The reaction mixture was allowed to stir for 1 h at rt, then the solvent was evaporated under reduced pressure. The crude was dissolved in HCl 1 M (30 mL), and the solvent was evaporated to afford the corresponding HCl salt (63 mg) as a white solid. The compound was recrystallized from MeOH/ CHCl_3 to afford the title compound as a white powder (51 mg, 46%). ^1H NMR (CDCl_3) δ (two rotamers) 9.64 (br s, 1H), 7.27–7.22 (m, 3H), 7.15–7.13 (m, 1H), 4.40 (d, $J = 5.5$ Hz, 0.4H), 4.25 (d, $J = 6.5$ Hz, 0.6H), 3.79–3.44 (m, 3H), 2.38–2.28 (m, 1H), 2.06–1.96 (m, 1H), 1.49 (s, 4H), 1.42 (s, 5H). ^{13}C NMR (CDCl_3) δ (two rotamers) 177.6, 175.7, 155.2, 153.7, 142.9, 142.4, 134.6, 130.1, 127.5, 127.4, 127.1, 125.2,

81.2, 80.1, 65.4, 64.9, 49.4, 47.5, 46.1, 45.9, 32.7, 32.2, 28.3, 28.2. MS (m/z) calcd. for $C_{12}H_{13}F_3NO_2$ $[M + H]^+$ 295.06, found 295.1. $[\alpha]_{25}^D$ +58.9 ($c = 0.38$, MeOH). Mp: 180.7–182.5 °C.

(2S,3R)-3-(3-Aminophenyl)pyrrolidine-2-carboxylic Acid Dihydrochloride (1f). Acid 7f (41 mg, 0.101 mmol, 1 equiv) was dissolved in a 1:1 mixture TFA/DCM (2.0 mL). The reaction mixture was allowed to stir for 1.5 h at rt, then the solvent was evaporated under reduced pressure. The oily residue was dissolved in 1 M HCl (10 mL), and the solvent was evaporated (3×) to give the crude product, which was recrystallized from MeOH/CHCl₃ to afford the title compound as a white solid (22 mg, 78%). ¹H NMR (MeOD) δ 7.58–7.31 (m, 3H), 7.31 (d, $J = 7.2$ Hz, 1H), 4.45 (d, $J = 9.1$ Hz, 1H), 3.77–3.58 (m, 2H), 3.57–3.42 (m, 1H), 2.66–2.49 (m, 1H), 2.36–2.17 (m, 1H). ¹³C NMR (CDCl₃) δ 168.5, 144.4, 140.6, 131.18, 131.17, 124.8, 118.6, 66.7, 49.6, 46.8, 34.4. MS (m/z) calcd. for $C_{11}H_{15}N_2O_2$ $[M + H]^+$ 207.1, found 207.1. $[\alpha]_{25}^D$ +62.7° ($c = 0.22$, MeOH). Mp: decomposition.

(2S,3R)-3-(3-Cyanophenyl)pyrrolidine-2-carboxylic Acid Hydrochloride (1g). Acid 7g (65 mg, 0.205 mmol, 1 equiv) was dissolved in a 1:1 mixture of TFA/DCM (2.0 mL). The reaction mixture was allowed to stir for 3 h at rt, then the solvent was evaporated under reduced pressure. The oily residue was dissolved in HCl 1 M (10 mL) and evaporated to dryness (3×) to afford the title compound as a white solid (42 mg, 81%). ¹H NMR (D₂O) δ 7.82 (t, $J = 1.6$ Hz, 1H), 7.78–7.70 (m, 2H), 7.59 (t, $J = 7.8$ Hz, 1H), 4.44 (d, $J = 9.9$ Hz, 1H), 3.80–3.68 (m, 2H), 3.57 (ddd, $J = 11.8$, 10.3, 6.9 Hz, 1H), 2.61 (dtd, $J = 10.5$, 7.1, 3.3 Hz, 1H), 2.35–2.22 (m, 1H). ¹³C NMR (D₂O + dioxane) δ 171.4, 140.3, 133.4, 132.5, 132.1, 130.5, 120.0, 112.3, 65.41, 48.0, 46.4, 33.4. LC–MS (m/z) calcd. for $C_{12}H_{13}N_2O_2$ $[M + H]^+$ 217.10, found 217.0. Mp: 210.8–212.9 °C.

(2S,3R)-3-(3-Carbamoylphenyl)-2-carboxypyrrolidin-1-ium Chloride (1h). H₂O₂ (4.23 mmol, 0.43 mL of 30% solution in H₂O, 6 equiv) was added dropwise to a solution of 7g (223 mg, 0.71 mmol, 1.0 equiv) and K₂CO₃ (390 mg, 2.82 mmol, 4 equiv) in EtOH/H₂O (1:1, 4.86 mL). The reaction mixture was stirred at rt for 70 min, then slowly acidified with 1 M HCl. The aqueous phase was extracted with EtOAc (3 × 10 mL) and the combined organic layers washed with brine (10 mL), dried over MgSO₄, and concentrated to give a pale yellow solid. The crude was dissolved in DCM (5.8 mL), and TFA (5.8 mL) was added. The reaction mixture was stirred for 2 h at rt. The solvent was evaporated, and the oily residue was dissolved in 1 M HCl and evaporated to dryness (3 × 10 mL). The crude pink solid was recrystallized from H₂O/acetone to afford the title compound as a white solid (95 mg, 59% over two steps). ¹H NMR (D₂O) δ 7.85 (d, $J = 1.6$ Hz, 1H), 7.83–7.77 (m, 1H), 7.70–7.65 (m, 1H), 7.59 (t, $J = 7.7$ Hz, 1H), 4.38 (d, $J = 9.7$ Hz, 1H), 3.77–3.67 (m, 2H), 3.64–3.52 (m, 1H), 2.61 (dtd, $J = 13.9$, 7.1, 3.4 Hz, 1H), 2.39–2.25 (m, 1H). ¹³C NMR (D₂O) δ 173.4, 172.3, 139.9, 134.1, 132.2, 130.1, 127.4, 127.2, 66.1, 48.7, 46.3, 33.7. LC–MS (m/z) calcd. for $C_{12}H_{15}N_2O_3$ $[M + H]^+$ 235.1, found 235.1. Mp: decomposition.

(2S,3R)-3-(3-Boronophenyl)pyrrolidine-2-carboxylic Acid Hydrochloride (1i). To a solution of 7i (50 mg, 0.120 mmol, 1.0 equiv) in acetone (9.4 mL) was added 0.1 M NH₄OAc (27.7 mg, 0.36 mmol, 3.0 equiv, in H₂O) and NaIO₄ (76.8 mg, 0.36 mmol, 3 equiv). The reaction mixture was stirred for 48 h at rt. Acetone was removed under reduced pressure, and the aqueous layer was diluted with 2 M NaOH (4 mL) and washed with EtOAc. The aqueous phase was then acidified with 1 M HCl until pH \approx 3 and extracted with EtOAc (4 × 5 mL). The combined organic layers were washed with brine (10 mL), dried over MgSO₄, and concentrated to dryness. The crude product was dissolved in DCM (1.0 mL) and TFA (1.0 mL), and the reaction mixture stirred for 2.5 h at rt. The solvents were evaporated, and the oily residue was dissolved in 1 M HCl and evaporated to dryness (3 × 10 mL) to give an off-white solid, which was recrystallized from H₂O/acetone to give the title compound as an off-white solid (13 mg, 43% over two steps). ¹H NMR (D₂O) δ 7.80–7.72 (m, 2H), 7.58–7.46 (m, 2H), 4.41 (d, $J = 9.8$ Hz, 1H), 3.75–3.65 (m, 2H), 3.56 (ddd, $J = 11.7$, 10.3, 6.9 Hz, 1H), 2.57 (dtd, $J = 13.9$, 7.1, 3.4 Hz, 1H), 2.38–2.20 (m, 1H). ¹³C NMR (D₂O + dioxane) δ 171.4, 137.9, 133.1, 132.6, 130.1,

128.7, 65.2, 48.2, 45.8, 33.1. LC–MS (m/z) calcd. for $C_{11}H_{15}BNO_4$ $[M + H]^+$ 236.1, found 236.1. Mp: decomposition.

(2S,3R)-3-(3,4-Dihydroxyphenyl)pyrrolidine-2-carboxylic Acid (1j). In a flame-dried flask a solution of 7j (70 mg, 0.21 mmol, 1.0 equiv) in dry DCM (3 mL) was cooled to 0 °C. A 1 M solution of BBr₃ (in DCM) (0.53 mL, 0.522 mmol, 2.5 equiv) was added dropwise, and the reaction mixture was allowed to stir 3 h at rt. The reaction mixture was quenched with H₂O (1 mL), and the solvent evaporated. The crude product was purified by preparative HPLC and then recrystallized from MeOH to afford the title compound as a white solid (3.8 mg, 8% yield). ¹H NMR (CDCl₃) δ 6.89–6.94 (m, 2H), 6.79–6.86 (m, 1H), 4.02 (d, $J = 9.03$ Hz, 1H), 3.54–3.62 (m, 1H), 3.36–3.51 (m, 2H), 2.43 (dtd, $J = 3.64$, 6.73, 13.52 Hz, 1H), 2.09–2.23 (m, 1H). MS (m/z) calcd. for $C_{11}H_{13}NO_4$ $[M + H]^+$ 224.09, found 224.1.

(2S,3R)-2-Carboxy-3-(3-carboxy-4-fluorophenyl)pyrrolidin-1-ium Chloride (1k). Acid 7k (85 mg, 0.24 mmol, 1 equiv) was dissolved in a 1:1 mixture TFA/DCM (4.66 mL). The reaction mixture was allowed to stir for 2 h at rt, then the solvent was evaporated under reduced pressure. The oily residue was dissolved in HCl 1 M (10 mL), and the solvent was evaporated (3×) to afford the title compound as a white solid (42 mg, 60%). ¹H NMR (D₂O, 400 MHz) δ 7.97 (dd, $J = 6.9$, 2.6 Hz, 1H), 7.69 (ddd, $J = 8.6$, 4.6, 2.5 Hz, 1H), 7.31 (dd, $J = 11.0$, 8.6 Hz, 1H), 4.36 (d, $J = 9.7$ Hz, 1H), 3.77–3.66 (m, 2H), 3.57 (ddd, $J = 11.8$, 10.2, 6.9 Hz, 1H), 2.59 (dtd, $J = 13.9$, 7.0, 3.3 Hz, 1H), 2.29 (dtd, $J = 13.4$, 10.4, 8.2 Hz, 1H). ¹³C NMR (D₂O) δ 172.0, 168.4, 162.5, 160.8, 135.34, 135.31, 135.2, 135.1, 131.5, 119.2, 119.1, 118.2, 118.1, 67.2, 65.9, 47.8, 46.3, 33.5. MS (m/z) calcd. for $C_{12}H_{13}FNO_4$ $[M + H]^+$ 254.1, found 254.1. Mp: 196.8 → dec.

(2S,3R)-3-(3-Carboxy-4-chlorophenyl)pyrrolidine-2-carboxylic Acid Hydrochloride (1l). Diacid 7l (190 mg, 0.514 mmol, 1 equiv) was dissolved in a 1:1 mixture TFA/DCM (10 mL). The reaction mixture was allowed to stir for 2 h at rt, then the solvent was evaporated under reduced pressure. The oily residue was dissolved in 1 M HCl (10 mL), and the solvent was evaporated (3 times) to afford the corresponding HCl salt (135 mg). The crude product was recrystallized from H₂O/acetone to afford the title compound as an off-white solid (89 mg, 56%). ¹H NMR (D₂O) δ 7.85 (d, $J = 1.8$ Hz, 1H), 7.68–7.49 (m, 2H), 4.37 (d, $J = 9.7$ Hz, 1H), 3.71 (ddd, $J = 11.8$, 9.2, 5.1 Hz, 2H), 3.62–3.52 (m, 1H), 2.60 (dtd, $J = 13.9$, 7.1, 3.4 Hz, 1H), 2.35–2.23 (m, 1H). ¹³C NMR (D₂O) δ 171.9, 170.7, 138.3, 132.6, 131.9, 131.8, 131.7, 130.3, 65.7, 47.8, 46.2, 33.4. MS (m/z) calcd. for $C_{12}H_{13}ClNO_4$ $[M + H]^+$ 270.0, found 270.0. Mp 239.4–241.3 °C.

(2S,3R)-3-(3-Carboxy-4-methylphenyl)pyrrolidine-2-carboxylic Acid Hydrochloride (1m). A solution of NaIO₄ (638 mg, 2.98 mmol, 8.2 equiv) and RuCl₃·xH₂O (4.5 mg, 0.022 mmol, 0.06 equiv) in H₂O (4.5 mL) was added to a solution of 6m (117 mg, 0.36 mmol) in MeCN/EtOAc (1:1, 5.2 mL) cooled to 0 °C. The reaction mixture was stirred for 30 min and then filtered through Celite, and the filter cake was washed with EtOAc. The aqueous layer was extracted with EtOAc, and the combined organic layers were washed with brine, dried over MgSO₄, and concentrated to give the corresponding diacid, which was used without further purification. The diacid 7m was dissolved in a 1:1 mixture of TFA/DCM (6.0 mL), the reaction mixture was allowed to stir for 2.5 h at rt, and the solvent was evaporated under reduced pressure. The oily residue was dissolved in 1 M HCl (10 mL) and evaporated to dryness (3×). The crude product was purified by preparative HPLC (0 to 40% B in A) and then evaporated with 1 M HCl (3 × 1 mL) to afford the title compound, as a white solid (21 mg, 20% over two steps). ¹H NMR (600 MHz, D₂O) δ 7.78 (d, $J = 2.0$ Hz, 1H), 7.45 (dd, $J = 7.9$, 2.1 Hz, 1H), 7.29 (d, $J = 7.9$ Hz, 1H), 4.39 (d, $J = 9.8$ Hz, 1H), 3.69–3.61 (m, 2H), 3.51 (ddd, $J = 11.7$, 10.2, 6.9 Hz, 1H), 2.50 (dtd, $J = 10.5$, 7.1, 3.2 Hz, 1H), 2.44 (s, 3H), 2.25–2.17 (m, 1H). ¹³C NMR (151 MHz, D₂O) δ 171.54, 170.63, 139.15, 135.72, 132.31, 131.28, 130.16, 129.04, 64.56, 47.25, 45.81, 32.82, 20.04. MS (m/z) calcd. for $C_{13}H_{16}NO_4$ $[M + H]^+$ 250.3, found 250.3. Mp: decomposition.

(2S,3R)-3-(3-Carboxy-4-bromophenyl)pyrrolidine-2-carboxylic Acid Hydrochloride (1n). ¹H NMR (600 MHz, D₂O) δ 7.67 (d, $J = 8.3$ Hz, 1H), 7.63 (d, $J = 2.3$ Hz, 1H), 7.36 (dd, $J = 8.3$, 2.4 Hz, 1H),

4.18 (d, $J = 9.4$ Hz, 1H), 3.61–3.54 (m, 1H), 3.48–3.43 (m, 1H), 2.51–2.46 (m, 1H), 2.21–2.14 (m, 1H). ^{13}C NMR (600 MHz, D_2O) δ 171.9, 171.6, 138.6, 134.8, 134.2, 131.4, 128.8, 118.4, 65.6, 47.5, 45.6, 32.8. MS (m/z) calcd. for $\text{C}_{12}\text{H}_{12}\text{BrNO}_4$ [$M + \text{H}$] $^+$ 312.9 and 314.9, found 313.9 and 315.9. Mp: 250.1–257.3 °C.

5-Bromo-2-methylbenzyl)oxy(tert-butyl)dimethylsilane (3m). To a flame-dried round-bottom flask was charged with 5-bromo-2-methylphenyl)methanol³⁵ (4.34 g, 21.6 mmol), anhydrous DMF (50 mL), imidazole (4.41 g, 64.8 mmol), TBSCl (6.51 g, 43.2 mmol), and DMAP (264 mg, 2.16 mmol). The reaction mixture was stirred for 16 h at rt and subsequently diluted with EtOAc. The resulting mixture was washed twice with 1 M HCl, twice with brine, dried over MgSO_4 , filtered, and concentrated *in vacuo*. The crude product was purified by consecutive flash chromatography (heptanes/EtOAc, 2:1 and 5:1) to provide title compound as a clear oil (4.63 g, 68%). ^1H NMR (600 MHz, CDCl_3) δ 7.56 (d, $J = 2.0$ Hz, 1H), 7.27 (dd, $J = 8.0, 2.2$ Hz, 1H), 6.98 (d, $J = 8.0$ Hz, 1H), 4.65 (s, 2H), 2.19 (s, 3H), 0.95 (s, 9H), 0.11 (s, 6H). ^{13}C NMR (151 MHz, CDCl_3) δ 141.60, 133.72, 131.50, 129.77, 129.30, 119.78, 62.76, 26.09, 18.56, 18.16, –5.17. R_f 0.84 (heptane/EtOAc, 1:1).

tert-Butyldimethyl((2-methyl-5-(4,4,5,5-tetramethyl-1,3,2-dioxaborolan-2-yl)benzyl)oxy)silane (3n). A dry, Ar-filled 20 mL vial was charged with bromine **3m** (419 mg, 1.33 mmol), $(\text{Bpin})_2$ (354 mg, 1.40 mmol), KOAc (394 mg, 4.06 mmol), and $(\text{PPh}_3)_2\text{PdCl}_2$ (46.9 mg, 66.5 μmol). The vial was then evacuated and backfilled with Ar, followed by addition of degassed dioxane (13.2 mL). The vial was capped with a screw cap and stirred for 16 h at 100 °C. The reaction mixture was then diluted with EtOAc and washed three times with H_2O . The organic partition was washed with brine, dried over MgSO_4 , filtered through Celite, and evaporated. The crude product was purified by DCVC (heptane/EtOAc, 10:1) to yield the title compound (407 mg, contains 5 mol % PPh_3), which was used without further purification. ^1H NMR (600 MHz, CDCl_3) δ 7.76 (s, 1H), 7.62 (dd, $J = 7.4, 1.0$ Hz, 1H), 7.15 (d, $J = 7.5$ Hz, 1H), 4.70 (s, 2H), 2.34 (s, 3H), 1.33 (s, 12H), 0.93 (s, 9H), 0.09 (s, 6H). ^{13}C NMR (151 MHz, CDCl_3) δ 139.94, 138.40, 134.16, 134.03, 129.75, 83.71, 64.14, 26.11, 25.01, 19.19, 18.57, –5.11. R_f 0.54 (heptane/EtOAc, 10:1).

(2S,3R)-tert-Butyl 2-(((tert-Butyldimethylsilyloxy)methyl)-3-(3-ethoxycarbonyl)phenyl)-5-oxopyrrolidine-1-carboxylate (4a). $[\text{Rh}(\text{cod})\text{Cl}]_2$ (37.6 mg, 0.076 mmol, 0.05 equiv), (S)-tert-butyl 2-(((tert-butylidimethylsilyloxy)methyl)-5-oxo-2,5-dihydro-1H-pyrrole-1-carboxylate (**2**) (500 mg, 1.53 mmol, 1.0 equiv) and 3-(ethoxycarbonyl)phenylboronic acid (**3a**, 474 mg, 2.44 mmol, 1.6 equiv) were placed in a 50 mL flask, which was evacuated and backfilled with N_2 . Degassed dioxane (13.0 mL) was added, and to the stirred clear solution, 1 M NaOH (2.44 mL, 1.6 equiv, degassed water) was added dropwise. The reaction mixture was stirred at rt for 4.5 h. The reaction mixture was diluted with H_2O , and the aqueous phase was extracted with EtOAc (3 \times 15 mL). The combined organic layers were washed with brine (1 \times 20 mL), dried over MgSO_4 , and concentrated to give 743 mg. The crude product was purified by flash chromatography (heptanes/EtOAc, 9:1) to afford the title compound as an off-white solid (382 mg, 52%). ^1H NMR (CDCl_3) δ 7.95 (dt, $J = 7.4, 1.6$ Hz, 1H), 7.87 (s, 1H), 7.39 (tt, $J = 4.6, 3.3$ Hz, 2H), 4.38 (q, $J = 7.1$ Hz, 2H), 4.09 (dt, $J = 4.0, 2.1$ Hz, 1H), 4.01 (dd, $J = 10.6, 3.9$ Hz, 1H), 3.82 (dd, $J = 10.5, 2.2$ Hz, 1H), 3.54 (dt, $J = 9.6, 2.4$ Hz, 1H), 3.17 (dd, $J = 17.9, 9.6$ Hz, 1H), 2.53 (dd, $J = 17.9, 2.8$ Hz, 1H), 1.53 (s, 9H), 1.39 (t, $J = 7.1$ Hz, 3H), 0.91 (s, 9H), 0.08 (s, 3H), 0.07 (s, 3H). ^{13}C NMR (CDCl_3) δ 173.7, 166.4, 150.0, 144.6, 131.4, 130.6, 129.4, 128.5, 128.0, 83.3, 66.6, 63.7, 61.3, 40.1, 38.8, 28.2, 26.0, 18.3, 14.5, –5.3. LC–MS (m/z) calcd. for $\text{C}_{25}\text{H}_{39}\text{NO}_6\text{Si}$ [$M + \text{H}$] $^+$ 478.2, found 378.2 [($M + \text{H}$)-Boc] $^+$. R_f 0.25 (heptanes/EtOAc, 8:2).

(2S,3R)-tert-Butyl 3-(3-Bromophenyl)-2-(((tert-Butyldimethylsilyloxy)methyl)-5-oxopyrrolidine-1-carboxylate (4b). To a solution at rt of (S)-tert-butyl 2-(((tert-butylidimethylsilyloxy)methyl)-5-oxo-2,5-dihydro-1H-pyrrole-1-carboxylate (**2**) (1.0 g, 3.05 mmol, 1.0 equiv) and 3-bromophenylboronic acid (**3b**, 981 mg, 4.89 mmol, 1.6 equiv) in degassed THF (26.3 mL) under nitrogen was added $[\text{Rh}(\text{cod})\text{Cl}]_2$ (75.3 mg, 0.153 mmol, 0.05 equiv). A 1 M NaOH (4.9 mL, 1.6 equiv) solution was then added dropwise, and the reaction mixture stirred at

rt for 4 h. The reaction mixture was diluted with H_2O , and the aqueous phase was extracted with EtOAc (3 \times 15 mL). The combined organic layers were washed with brine (1 \times 20 mL), dried over MgSO_4 , and concentrated to give 1.56 g. The crude product was purified by flash chromatography (heptanes/EtOAc, 9:1) to afford the title compound as a white solid (803 mg, 54%). ^1H NMR (CDCl_3 , 400 MHz) δ 7.40 (ddd, $J = 7.9, 1.9, 1.0$ Hz, 1H), 7.34 (t, $J = 1.8$ Hz, 1H), 7.21 (t, $J = 7.8$ Hz, 1H), 7.14–7.09 (m, 1H), 4.06 (dt, $J = 3.9, 2.0$ Hz, 1H), 3.99 (dd, $J = 10.5, 3.9$ Hz, 1H), 3.80 (dd, $J = 10.5, 2.2$ Hz, 1H), 3.42 (dt, $J = 9.6, 2.2$ Hz, 1H), 3.14 (dd, $J = 17.9, 9.6$ Hz, 1H), 2.50 (dd, $J = 17.9, 2.6$ Hz, 1H), 1.53 (s, 9H), 0.91 (s, 9H), 0.08 (s, 3H), 0.07 (s, 3H). ^{13}C NMR (CDCl_3 , 400 MHz) δ 173.6, 150.0, 146.6, 130.8, 130.5, 129.9, 125.0, 123.2, 83.4, 66.6, 63.8, 39.94, 38.7, 28.2, 26.0, 18.3, –5.3, –5.4. R_f 0.21 (heptanes/EtOAc, 9:1).

(2S,3R)-tert-Butyl-2-(((tert-Butyldimethylsilyloxy)methyl)-3-(3-chlorophenyl)-5-oxopyrrolidine-1-carboxylate (4d). To a solution of (S)-tert-butyl 2-(((tert-butylidimethylsilyloxy)methyl)-5-oxo-2,5-dihydro-1H-pyrrole-1-carboxylate (**2**) (500 mg, 1.53 mmol, 1.0 equiv) and 3-(chlorophenyl)boronic acid (**3d**, 382 mg, 2.44 mmol, 1.6 equiv) in THF/ H_2O (9:1, 15 mL) under nitrogen at rt was added $[\text{Rh}(\text{cod})\text{Cl}]_2$ (37.6 mg, 0.076 mmol, 0.05 equiv). Then, 1 M NaOH (2.5 mL, 1.6 equiv) was added dropwise, and the reaction mixture was stirred at rt for 4.5 h. The reaction mixture was diluted with H_2O , and the aqueous phase was extracted with EtOAc (3 \times 15 mL). The combined organic layers were washed with brine (1 \times 20 mL), dried over MgSO_4 , and concentrated to give 690 mg. The crude product was purified by flash chromatography (heptanes/EtOAc, 4:1) to afford the title compound as a white solid (387 mg, 58%). ^1H NMR (CDCl_3) δ 7.55–7.38 (m, 4H, Ar–H), 4.09 (m, 1H, CH–N), 4.01 (m, 1H), 3.83 (dd, $J = 10.5, 2.3$ Hz, 1H), 3.54 (dt, $J = 9.5, 2.3$ Hz, 1H), 3.20 (dd, $J = 17.9, 9.7$ Hz, 1H), 2.53 (dd, $J = 17.8, 2.5$ Hz, 1H), 1.54 (s, 9H), 0.92 (s, 9H), 0.09 (s, 3H), 0.08 (s, 3H). ^{13}C NMR (CDCl_3) δ 173.3, 149.8, 145.1, 131.3 (q, $J = 32$ Hz, C–CF₃), 129.7, 129.4, 124.0 (q, $J = 3.7$ Hz, C–Ar), 123.9 (q, $J = 270$ Hz, CF₃), 123.6 (q, $J = 3.7$, C–Ar), 83.3, 66.3, 63.3, 39.8, 38.7, 28.0, 25.8, 18.1, –5.5, –5.6. LC–MS (m/z) calcd. for $\text{C}_{22}\text{H}_{35}\text{ClNO}_4\text{Si}$ [$M + \text{H}$] $^+$ 440.2, found 340.1 [($M + \text{H}$)-Boc] $^+$. [α]₂₅^D –26.5 ($c = 0.27$, MeOH). Mp: 71.4–73.9 °C. R_f 0.29 (heptanes/EtOAc, 9:1).

(2S,3R)-tert-Butyl 2-(((tert-Butyldimethylsilyloxy)methyl)-5-oxo-3-(3-(trifluoromethyl)phenyl)pyrrolidine-1-carboxylate (4e). To a solution of (S)-tert-butyl 2-(((tert-butylidimethylsilyloxy)methyl)-5-oxo-2,5-dihydro-1H-pyrrole-1-carboxylate (**2**) (1.0 g, 3.053 mmol, 1 equiv) and commercially available 3-(trifluoromethyl)phenylboronic acid (**3e**, 928 mg, 4.89 mmol, 1.6 equiv) in THF/ H_2O (9:1, 30.0 mL) under nitrogen at rt was added $[\text{Rh}(\text{cod})\text{Cl}]_2$ (75.3 mg, 0.153 mmol, 0.05 equiv). Then, 1 M NaOH (5.0 mL, 1.6 equiv) was added dropwise, and the reaction mixture was stirred at rt for 4 h. The reaction mixture was diluted with H_2O , and the aqueous phase was extracted with EtOAc (3 \times 20 mL). The combined organic layers were washed with brine (1 \times 30 mL), dried over MgSO_4 , and concentrated. The crude product was purified by flash chromatography (heptanes/EtOAc, 9:1) to afford the title compound as a white solid (727 mg, 56%). ^1H NMR (CDCl_3) δ 7.55–7.38 (m, 4H), 4.09 (m, 1H), 4.01 (m, 1H), 3.83 (dd, $J = 10.5, 2.3$ Hz, 1H), 3.54 (dt, $J = 9.5, 2.3$ Hz, 1H), 3.20 (dd, $J = 17.9, 9.7$ Hz, 1H), 2.53 (dd, $J = 17.8, 2.5$ Hz, 1H), 1.54 (s, 9H), 0.92 (s, 9H), 0.09 (s, 3H), 0.08 (s, 3H). ^{13}C NMR (CDCl_3) δ 173.3, 149.8, 145.1, 131.3 (q, $J = 32$ Hz), 129.7, 129.4, 124.0 (q, $J = 3.7$ Hz), 123.9 (q, $J = 270$ Hz), 123.6 (q, $J = 3.7$ Hz), 83.3, 66.3, 63.3, 39.8, 38.7, 28.0, 25.8, 18.1, –5.5, –5.6. LC–MS (m/z) calcd. for $\text{C}_{23}\text{H}_{35}\text{F}_3\text{NO}_4\text{Si}$ [$M + \text{H}$] $^+$ 474.2, found 374.1 [($M + \text{H}$)-Boc] $^+$. [α]₂₅^D –26.4 ($c = 0.32$, MeOH). Mp: 95.3–96.9 °C. R_f 0.29 (heptanes/EtOAc, 9:1).

(2S,3R)-tert-Butyl 3-(3-((tert-Butoxycarbonyl)amino)phenyl)-2-(((tert-butylidimethylsilyloxy)methyl)-5-oxopyrrolidine-1-carboxylate (4f). $[\text{Rh}(\text{cod})\text{Cl}]_2$ (37.6 mg, 0.076 mmol, 0.05 equiv), (S)-tert-butyl 2-(((tert-butylidimethylsilyloxy)methyl)-5-oxo-2,5-dihydro-1H-pyrrole-1-carboxylate (500 mg, 1.53 mmol, 1.0 equiv), and 3-(tert-butoxycarbonylamino)boronic acid (**3f**, 579 mg, 2.44 mmol, 1.6 equiv) were placed in a 50 mL flask, which was evacuated and backfilled with N_2 . Degassed dioxane (13.0 mL) was added followed by dropwise

addition of 1 M NaOH (2.44 mL, 1.6 equiv, degassed water). The reaction mixture was stirred at rt for 3.5 h. The reaction mixture was diluted with H₂O, and the aqueous phase was extracted with EtOAc (3 × 15 mL). The combined organic layers were washed with brine (1 × 20 mL), dried over MgSO₄, and concentrated to give 743 mg. The crude product was purified by flash chromatography (heptanes/EtOAc, 9:1) to afford the title compound as a pale yellow oil (471 mg, 59% yield). ¹H NMR (CDCl₃) δ 7.19–7.30 (m, 3H), 6.82–6.90 (m, 1H), 6.49 (s, 1H), 4.07–4.12 (m, 1H), 4.02 (dd, *J* = 3.51, 10.54 Hz, 1H), 3.80 (dd, *J* = 1.88, 10.67 Hz, 1H), 3.43 (td, *J* = 1.88, 9.54 Hz, 1H), 3.15 (dd, *J* = 9.54, 17.82 Hz, 1H), 2.50 (dd, *J* = 2.26, 17.82 Hz, 1H), 1.52 (s, 9H), 0.91 (s, 9H), 0.08 (s, 3H), 0.07 (s, 3H). ¹³C NMR (CDCl₃) δ 174.1, 152.6, 149.9, 145.4, 138.9, 129.7, 120.7, 117.2, 116.6, 83.0, 80.7, 66.6, 63.8, 40.2, 38.9, 28.3, 28.1, 25.8, 18.2, –5.5. LC–MS (*m/z*) calcd. for C₂₇H₄₃N₂O₆Si [M + H]⁺ 521.3, found 365.2 [(M + H)–Boc-*t*-Bu]. [α]₂₅^D –19.8 (*c* = 0.55, MeOH). R_f 0.28 (heptanes/EtOAc, 8:2).

(2*S*,3*R*)-*tert*-Butyl 3-(Benzo[*d*][1,3]dioxol-5-yl)-2-(((*tert*-butyldimethylsilyloxy)methyl)-3-(3-(((*tert*-butyldimethylsilyloxy)methyl)-5-oxopyrrolidine-1-carboxylate (4j)). [Rh(cod)Cl]₂ (112.9 mg, 0.229 mmol, 0.05 equiv) was added to a solution of (*S*)-*tert*-butyl 2-(((*tert*-butyldimethylsilyloxy)methyl)-5-oxo-2,5-dihydro-1*H*-pyrrole-1-carboxylate (2) (1.50 g, 4.58 mmol, 1.0 equiv) and benzo[*d*][1,3]dioxol-5-ylboronic acid (1.22 g, 7.33 mmol, 1.6 equiv) in THF (39.0 mL) under nitrogen at rt. Aqueous 1 M NaOH (7.5 mL, 1.6 equiv) was then added dropwise, and the reaction mixture was stirred at rt for 4 h. The reaction mixture was diluted with H₂O, and the aqueous phase was extracted with EtOAc (3 × 30 mL). The combined organic layers were washed with brine (1 × 50 mL), dried over MgSO₄, and concentrated. The crude product was purified by flash chromatography (heptanes/EtOAc, 9:1) to afford the title compound as a white solid (1.38 g, 67%). ¹H NMR (CDCl₃) δ 6.75 (d, *J* = 8.0 Hz, 1H), 6.68 (d, *J* 1.8 Hz, 1H), 6.64 (dd, *J* = 8.0, 1.8 Hz, 1H), 5.95 (s, 2H), 4.03 (m, 1H), 3.98 (m, 1H), 3.78 (dd, *J* = 10.4, 2.1 Hz, 1H), 3.37 (dt, *J* = 9.5, 2.3 Hz, 1H), 3.12 (dd, *J* = 17.8, 9.5 Hz, 1H), 2.47 (dd, *J* = 17.8, 2.8 Hz, 1H), 1.53 (s, 9H), 0.91 (s, 9H), 0.08 (s, 3H), 0.07 (s, 3H). ¹³C NMR (CDCl₃) δ 173.9, 149.8, 148.2, 146.6, 138.1, 119.3, 108.5, 106.7, 101.1, 83.0, 66.9, 63.5, 40.2, 38.5, 28.1, 25.8, 18.2, –5.5. LC–MS (*m/z*) calcd. for C₂₃H₃₆NO₆Si [M + H]⁺ 450.2, found 350.1 [(M + H)–Boc]⁺. [α]₂₅^D –25.6 (*c* = 0.42, MeOH). Mp: 106.6–107.6 °C. R_f 0.36 (heptanes/EtOAc, 8:2).

(2*S*,3*R*)-*tert*-Butyl 2-(((*tert*-butyldimethylsilyloxy)methyl)-3-(3-(((*tert*-butyldimethylsilyloxy)methyl)-4-fluorophenyl)-5-oxopyrrolidine-1-carboxylate (4k)). A flamed-dry round-bottomed flask was charged with a solution of *tert*-BuLi in pentane (8.98 mL, 15.265 mmol, 5.0 equiv) and cooled to –78 °C. A solution of bromine 3k (2.44 g, 7.634 mmol, 2.5 equiv) in dry Et₂O (25 mL) was added dropwise, and the clear, yellow solution was stirred at –78 °C for 10 min. A suspension of CuCN in dry Et₂O (2.5 mL) was added portion-wise at –78 °C. The resulting suspension was stirred at –78 °C for 5 min and then at –42 °C for 10 min (clear solution), after which it was recooled to –78 °C. Enone 2 was dissolved in dry Et₂O (3.0 mL) and added dropwise to the cuprate mixture at –78 °C, which resulted in a color change to bright dark red. The temperature was raised to –42 °C, and the reaction mixture was stirred at this temperature for 1 h. The brown solution was quenched by addition of a freshly prepared sat. NaHCO₃ (5 mL), allowed to warm up to rt, and then transferred to a separating funnel with water (15 mL) and EtOAc (15 mL). The organic layer was separated, and the aqueous layer was extracted with EtOAc (2 × 15 mL). The combined organic layers were washed with brine (1 × 15 mL), dried over anhydrous MgSO₄, filtered, and evaporated *in vacuo* to dryness. The crude product was purified by column chromatography (heptanes/EtOAc, 9:1) to afford the title compound as a pale yellow oil (793 mg, 1.40 mmol, 46% yield). ¹H NMR (CDCl₃) δ 7.30 (dd, *J* = 6.8, 2.3 Hz, 1H), 7.04 (ddd, *J* = 7.5, 4.9, 2.5 Hz, 1H), 6.95 (dd, *J* = 9.6, 8.5 Hz, 1H), 4.77 (s, 2H), 4.04 (dd, *J* = 3.9, 2.0 Hz, 1H), 3.99 (dd, *J* = 10.4, 4.0 Hz, 1H), 3.79 (dd, *J* = 10.4, 2.1 Hz, 1H), 3.45 (dt, *J* = 9.6, 2.3 Hz, 1H), 3.13 (dd, *J* = 17.9, 9.6 Hz, 1H), 2.49 (dd, *J* = 17.9, 2.7 Hz, 1H), 1.52 (s, 9H), 0.94 (s, 9H), 0.91 (s, 9H), 0.11 (s, 3H), 0.11 (s, 3H), 0.08 (s, 3H), 0.07 (s, 3H). ¹³C NMR (CDCl₃) δ 173.9, 159.8, 158.1, 150.0, 140.12, 140.10, 129.2, 129.1,

126.64, 126.61, 126.25, 126.19, 115.6, 115.4, 83.2, 66.9, 63.7, 59.1, 59.0, 40.3, 38.3, 28.2, 26.1, 26.0, 18.6, 18.3, –5.17, –5.20, –5.3. R_f 0.32 (heptanes/EtOAc, 9:1).

(2*S*,3*R*)-*tert*-Butyl 2-(((*tert*-butyldimethylsilyloxy)methyl)-3-(3-(((*tert*-butyldimethylsilyloxy)methyl)-4-chlorophenyl)-5-oxopyrrolidine-1-carboxylate (4l)). A flamed-dry round-bottomed flask was charged with a solution of *tert*-BuLi in pentane (8.98 mL, 15.265 mmol, 5.0 equiv) and cooled to –78 °C. A solution of 3l (2.56 g, 7.63 mmol, 2.5 equiv) in dry Et₂O (25 mL) was added dropwise, and the clear, yellow/orange solution was stirred at –78 °C for 10 min. A suspension of CuCN in dry Et₂O (2.4 mL) was added portion-wise at –78 °C. The resulting suspension was stirred at –78 °C for 5 min and then at –42 °C for 10 min (clear solution), after which it was recooled to –78 °C. Enone 2 was dissolved in dry Et₂O (3.0 mL) and added dropwise to the cuprate mixture at –78 °C, which resulted in a color change to bright dark red. The temperature was raised to –42 °C, and the reaction mixture was stirred at this temperature for 1 h. The brown solution was quenched by addition of a freshly prepared sat. NaHCO₃ (5 mL), allowed to warm up to rt, and then transferred to a separating funnel with water (15 mL) and EtOAc (15 mL). The organic layer was separated, and the aqueous layer was extracted with EtOAc (2 × 15 mL). The combined organic layers were washed with brine (1 × 15 mL), dried over anhydrous MgSO₄, filtered, and evaporated *in vacuo* to dryness. The crude product was purified by column chromatography (heptanes/EtOAc, 9:1) to afford the title compound as a low-melting white solid (1.31 g, 73%). ¹H NMR (CDCl₃) δ 7.39 (d, *J* = 2.3 Hz, 1H), 7.26 (d, *J* = 8.2 Hz, 1H), 7.01 (dd, *J* = 8.2, 2.3 Hz, 1H), 4.77 (s, 2H), 4.04 (dt, *J* = 3.9, 2.0 Hz, 1H), 4.00 (dd, *J* = 10.4, 3.9 Hz, 1H), 3.78 (dd, *J* = 10.4, 2.0 Hz, 1H), 3.45 (dt, *J* = 9.6, 2.3 Hz, 1H), 3.14 (dd, *J* = 17.9, 9.6 Hz, 1H), 2.50 (dd, *J* = 17.9, 2.8 Hz, 1H), 1.52 (s, 9H), 0.96 (s, 9H), 0.90 (s, 9H), 0.13 (s, 3H), 0.13 (s, 3H), 0.07 (s, 3H), 0.06 (s, 3H). ¹³C NMR (CDCl₃) δ 173.7, 150.0, 143.1, 139.6, 130.2, 129.6, 125.9, 125.8, 83.2, 66.7, 63.7, 62.4, 40.1, 38.6, 28.2, 26.1, 26.0, 18.6, 18.4, –5.1, –5.2, –5.34, –5.35. R_f 0.47 (heptanes/EtOAc, 8:2).

tert-Butyl (2*S*,3*R*)-2-(((*tert*-butyldimethylsilyloxy)methyl)-3-(3-(((*tert*-butyldimethylsilyloxy)methyl)-4-methylphenyl)-5-oxopyrrolidine-1-carboxylate (4m)). [Rh(cod)Cl]₂ (23.2 mg, 0.047 mmol, 0.05 equiv), (*S*)-*tert*-butyl 2-(((*tert*-butyldimethylsilyloxy)methyl)-5-oxo-2,5-dihydro-1*H*-pyrrole-1-carboxylate (2) (300 mg, 0.92 mmol), *tert*-butyldimethyl((2-methyl-5-(4,4,5,5-tetramethyl-1,3,2-dioxaborolan-2-yl)benzyl)oxy)silane (3n) (532 mg, 1.47 mmol), and Cs₂CO₃ (477 mg, 1.46 mmol) were placed in a 25 mL flask, which was evacuated and backfilled with Ar. Degassed, anhydrous THF (8.9 mL) was added, followed by addition of degassed H₂O (21 μL, 1.1 mmol). The reaction mixture was stirred at rt for 24 h. The reaction mixture was diluted with H₂O, and the aqueous phase was extracted with EtOAc (3 × 15 mL). The combined organic layers were washed with brine, dried over MgSO₄, and concentrated. The crude product was purified by flash chromatography (heptane:EtOAc, 10:1 to 5:2) to afford the title compound as a pale yellow oil (211 mg, 41% yield). ¹H NMR (400 MHz, CDCl₃) δ 7.24 (d, *J* = 1.4 Hz, 1H), 7.09 (d, *J* = 7.8 Hz, 1H), 7.00 (dd, *J* = 7.7, 2.0 Hz, 1H), 4.68 (s, 2H), 4.11–4.05 (m, 1H), 4.01 (dd, *J* = 10.5, 3.8 Hz, 1H), 3.79 (dd, *J* = 10.5, 2.0 Hz, 1H), 3.46–3.41 (m, 1H), 3.13 (dd, *J* = 17.9, 9.6 Hz, 1H), 2.53 (dd, *J* = 17.8, 2.8 Hz, 1H), 2.25 (s, 3H), 1.52 (s, 9H), 0.94 (s, 9H), 0.91 (s, 9H), 0.11 (s, 3H), 0.10 (s, 3H), 0.08 (s, 3H), 0.07 (s, 3H). ¹³C NMR (101 MHz, CDCl₃) δ 174.29, 150.02, 141.83, 139.94, 134.14, 130.65, 124.93, 124.83, 82.97, 67.01, 63.70, 63.41, 40.18, 38.57, 28.19, 26.08, 25.97, 18.52, 18.32, 18.26, –5.14, –5.15, –5.38, –5.40. R_f 0.43 (heptanes/EtOAc, 5:1).

(2*S*,3*R*)-*tert*-Butyl 3-(3-Chlorophenyl)-2-(hydroxymethyl)-pyrrolidine-1-carboxylate (6d). In a flame-dried flask a solution of 4d (368 mg, 0.84 mmol, 1.0 equiv) in dry THF (2.2 mL) was cooled to –78 °C. LiBEt₃H 1 M (1.0 mL, 1.00 mmol, 1.2 equiv) was added via syringe dropwise, and the reaction mixture was stirred for 1 h, quenched with NaHCO₃ sat. sol. (3 mL), and warmed to rt. The aqueous phase was extracted with EtOAc (3 × 5 mL), and the combined organic layers were washed with brine (10 mL), dried over MgSO₄, and concentrated to give the corresponding hemiaminal 5d as

a colorless oil, which was used in the next step without further purification.

In a flame-dried flask a solution of the crude hemiaminal **5d** (0.84 mmol, 1.0 equiv) in dry DCM (2.6 mL) was cooled to -78°C . HSiEt_3 (0.27 mL, 1.670 mmol, 2 equiv) and $\text{BF}_3\cdot\text{Et}_2\text{O}$ (0.23 mL, 1.837 mmol, 2.2 equiv) were added sequentially via syringe, and the reaction mixture stirred for 6 h. The reaction mixture was quenched with sat. NaHCO_3 (4 mL) and warmed to rt. The mixture was diluted with DCM, and the organic phase was separated, washed with sat. NH_4Cl (5 mL), dried over MgSO_4 , and concentrated. The crude product was purified by flash chromatography (heptanes/EtOAc, 2:1) to afford the title compounds as a colorless gummy oil (154 mg, 59% over two steps). ^1H NMR (CDCl_3) δ 7.31–7.26 (m, 3H, Ar–H), 7.16–7.14 (m, 1H, Ar–H), 3.94 (m, 1H, CH–N), 3.78 (m, 1H), 3.67 (m, 1H), 3.40 (m, 1H), 3.05 (broad s, 1H), 2.20 (m, 1H), 1.97 (m, 1H), 1.54 (s, 9H). ^{13}C NMR (CDCl_3) δ 156.5, 143.0, 134.5, 130.0, 127.6, 127.2, 125.7, 80.5, 66.7, 65.5, 47.2, 46.8, 32.6, 28.4. MS (m/z) calcd. for $\text{C}_{16}\text{H}_{23}\text{ClNO}_3$ $[\text{M} - \text{H}]^+$ 312.14, found 212.1 $[(\text{M} + \text{H})\text{-Boc}]^+$. $[\alpha]_{25}^{\text{D}}$ -13.1 ($c = 0.92$, MeOH). R_f 0.49 (heptanes/EtOAc, 1:1 + 1% AcOH).

(2S,3R)-tert-Butyl 2-(Hydroxymethyl)-5-oxo-3-(3-(trifluoromethyl)phenyl)pyrrolidine-1-carboxylate (6e). In a flame-dried flask a solution of **4e** (500 mg, 1.06 mmol, 1.0 equiv) in dry THF (2.8 mL) was cooled to -78°C . LiBEtH_3 1 M (solution in THF) (1.27 mL, 1.27 mmol, 1.2 equiv) was added via syringe dropwise, and the reaction mixture was stirred for 40 min, quenched with NaHCO_3 sat. sol. (3 mL), and warmed to rt. The aqueous phase was extracted with EtOAc (3×10 mL), and the combined organic layers were washed with brine (10 mL), dried over MgSO_4 , and concentrated to give the corresponding hemiaminal **5e** as a colorless oil, which was used in the next step without further purification.

In a flame-dried flask, a solution of the crude hemiaminal **5e** (1.06 mmol, 1 equiv) in dry DCM (3.3 mL) was cooled to -78°C . HSiEt_3 (0.34 mL, 2.11 mmol, 2 equiv) and $\text{BF}_3\cdot\text{Et}_2\text{O}$ (0.29 mL, 2.315 mmol, 2.2 equiv) were sequentially added via syringe, and the reaction mixture was stirred for 6 h. After the complete consumption of the substrate, the reaction was quenched with sat. NaHCO_3 (4 mL) and warmed to rt. The mixture was diluted with DCM, and the organic phase was separated, washed with sat. NH_4Cl (5 mL), dried over MgSO_4 , and concentrated to give 371 mg (crude). The crude was purified by flash chromatography (heptanes/EtOAc, 2:1) to afford the title compound as a colorless gummy oil (286 mg, 78% yield over two steps). ^1H NMR (CDCl_3) δ 7.49–7.39 (m, 4H), 4.94 (br s, 1H, OH), 3.92 (br s, 1H), 3.75–3.58 (m, 3H), 3.35 (ddd, $J = 11.2, 8.9, 6.8$, 1H), 3.04 (m, 1H), 2.18 (br s, 1H), 1.99–1.89 (m, 1H), 1.46 (s, 9H). ^{13}C NMR (CDCl_3) δ (two rotamers) 156.3, (154.3), (143.9), 142.1, 130.9 ($q, J = 31.5$ Hz, $\text{C}-\text{CF}_3$), 130.8, 129.1, 124.1, 123.9 ($q, J = 272.2$ Hz, CF_3), 123.8, 80.4, (80.1), 66.6, (65.6), 65.0, (62.5), 47.1, 46.7, (46.2), (32.6), 31.7. MS (m/z) calcd. for $\text{C}_{17}\text{H}_{23}\text{F}_3\text{NO}_3$ $[\text{M} + \text{H}]^+$ 346.2, found 246.1 $[(\text{M} + \text{H})\text{-Boc}]^+$. $[\alpha]_{25}^{\text{D}}$ -10.3 ($c = 0.43$, MeOH). R_f 0.23 (heptanes/EtOAc, 2:1).

(2S,3R)-tert-Butyl 3-(3-((tert-Butoxycarbonyl)amino)phenyl)-2-(hydroxymethyl)pyrrolidine-1-carboxylate (6f). In a flame-dried flask a solution of **4f** (371 mg, 0.71 mmol, 1.0 equiv) in dry THF (1.86 mL) was cooled to -78°C . LiBEtH_3 1 M (solution in THF) (1.7 mL, 1.72 mmol, 2.4 equiv) was added via syringe dropwise, and the reaction mixture was stirred for 1 h, quenched with sat. NaHCO_3 (3 mL), and warmed to rt. The aqueous phase was extracted with EtOAc (3×5 mL), and the combined organic layers were washed with brine (10 mL), dried over MgSO_4 , and concentrated to give the corresponding hemiaminal **4f** as a colorless oil, which was used in the next step without further purification.

In a flame-dried flask a solution of the crude hemiaminal **4f** (0.714 mmol, 1 equiv) in dry DCM (2.2 mL) was cooled to -78°C . HSiEt_3 (0.23 mL, 1.43 mmol, 2.0 equiv) and $\text{BF}_3\cdot\text{Et}_2\text{O}$ (0.27 mL, 2.14 mmol, 3.0 equiv) were sequentially added via syringe, and the reaction mixture was stirred for 5 h. After the complete consumption of the substrate, the reaction was quenched with NaHCO_3 sat. sol. (4 mL) and warmed to rt. The mixture was diluted with DCM, and the organic phase was separated, washed with sat. NH_4Cl (5 mL), dried over MgSO_4 , and concentrated. The crude product was purified by flash

chromatography (heptanes/EtOAc, 2:1) to afford the title compound as a colorless oil (110 mg, 31% over two steps). ^1H NMR (CDCl_3) δ 7.39 (s, 1H), 7.21 (t, $J = 7.8$ Hz, 1H), 7.12 (d, $J = 8.1$ Hz, 1H), 6.89 (d, $J = 7.6$ Hz, 1H), 6.57 (s, 1H), 3.90 (d, $J = 6.8$ Hz, 1H), 3.79–3.68 (m, 2H), 3.60 (dd, $J = 11.5, 6.7$ Hz, 1H), 3.39–3.27 (m, 1H), 2.92 (s, 1H), 2.14 (dtd, $J = 9.1, 6.5, 2.8$ Hz, 1H), 1.96 (dtd, $J = 12.4, 10.1, 8.1$ Hz, 1H), 1.51 (s, 9H), 1.49 (s, 9H). ^{13}C NMR (CDCl_3) δ 152.8, 141.1 (b), 139.0, 129.4, 122.3, 117.7, 117.4, 80.7, 80.6, 67.0, 48.0, 47.2, 32.9, 28.6, 28.5. MS (m/z) calcd. for $\text{C}_{21}\text{H}_{32}\text{N}_2\text{O}_5$ $[\text{M} + \text{H}]^+$ 392.23, found 293.1 $[(\text{M}-\text{Boc}) + \text{H}]^+$. $[\alpha]_{25}^{\text{D}}$ -8.6 ($c = 0.31$, MeOH). R_f 0.16 (heptanes/EtOAc, 2:1).

(2S,3R)-tert-Butyl 3-(3-Cyanophenyl)-2-(hydroxymethyl)pyrrolidine-1-carboxylate (6g). Under nitrogen atmosphere, TBAF (1.74 mmol, 3 equiv, 1.74 mL of 1 M solution in THF) was added to a solution of **8g** (242 mg, 0.581 mmol, 1 equiv) in dry THF (5.6 mL). The reaction mixture was stirred at rt for 2 h, then diluted with water (10 mL) and sat. NaHCO_3 (10 mL). The aqueous layer was extracted with EtOAc (2×10 mL), and the combined organic layers were washed with brine, dried over MgSO_4 , and concentrated. The crude product was purified by column chromatography (heptanes/EtOAc, 1:1) to give the title compound as a pale yellow oil (202 mg, 63% yield over two steps). ^1H NMR (CDCl_3) δ 7.51–7.34 (m, 4H), 4.78 (br s, 1H), 3.86 (br s, 1H), 3.73–3.54 (m, 3H), 3.33 (ddd, $J = 11.1, 8.8, 6.8$ Hz, 1H), 3.01 (bs, 1H), 2.17 (m, 1H), 1.95–1.81 (m, 1H), 1.43 (s, 9H). ^{13}C NMR (CDCl_3) δ 156.2, 154.2, 144.6, 142.9, 132.0, 131.1, 130.7, 129.6, 118.6, 112.7, 80.6, 80.3, 66.5, 65.5, 64.9, 62.4, 46.9, 46.8, 46.3, 32.5, 31.7, 28.4. R_f 0.21 (heptanes/EtOAc, 1:1).

(2S,3R)-tert-Butyl 2-(Hydroxymethyl)-3-(3-(4,4,5,5-tetramethyl-1,3,2-dioxaborolan-2-yl)phenyl)pyrrolidine-1-carboxylate (6i). Under nitrogen atmosphere, TBAF (1.311 mmol, 3 equiv, 1.31 mL of 1 M solution in THF), was added to a solution of **9** (226 mg, 0.437 mmol, 1 equiv) in dry THF (5.3 mL). The reaction mixture was stirred at rt for 2.5 h, then was diluted with sat. NaHCO_3 (10 mL). The aqueous layer was extracted with EtOAc (3×10 mL), and the combined organic layers were washed with brine, dried over MgSO_4 , and concentrated. The crude product was purified by column chromatography (heptanes/EtOAc, 2:1) to give the title compound as a colorless oil (106 mg, 63%). ^1H NMR (CDCl_3) δ 7.72–7.63 (m, 2H), 7.32–7.29 (m, 2H), 3.96 (bs, 1H), 3.72 (m, 2H), 3.59 (dd, $J = 11.5, 6.7$ Hz, 1H), 3.33 (td, $J = 10.5, 6.5$ Hz, 1H), 2.89 (bs, 1H), 2.10 (bs, 1H), 2.04–1.89 (m, 1H), 1.48 (s, 9H), 1.33 (s, 12H). ^{13}C NMR (CDCl_3) δ 156.9, 139.9, 133.9, 133.7, 130.7, 129.6, 128.2, 83.9, 80.5, 67.1, 66.0, 48.0, 47.2, 33.1, 28.5, 24.9. LC–MS (m/z) calcd. for $\text{C}_{17}\text{H}_{23}\text{N}_2\text{O}_3$ $[\text{M} + \text{H}]^+$ 302.17, found 203.1 $[(\text{M} + \text{H})\text{-Boc}]^+$. R_f 0.17 (heptanes/EtOAc, 2:1).

(2S,3R)-tert-Butyl 3-(Benzo[d][1,3]dioxol-5-yl)-2-(hydroxymethyl)-5-oxopyrrolidine-1-carboxylate (6j). In a flame-dried flask a solution of **4j** (687 mg, 1.53 mmol, 1.0 equiv) in dry THF (4 mL) was cooled to -78°C . LiBEtH_3 1 M (THF solution) (1.83 mL, 1.834 mmol, 1.2 equiv) was added via syringe dropwise, and the reaction mixture was stirred for 45 min, quenched with NaHCO_3 sat. sol. (4 mL), and warmed to rt. The aqueous phase was extracted with EtOAc (3×10 mL), and the combined organic layers were washed with brine (10 mL), dried over MgSO_4 , and concentrated to give the corresponding hemiaminal **5j** as a colorless oil, which was used in the next step without further purification.

In a flame-dried flask a solution of the crude hemiaminal (1.53 mmol, 1 equiv) in dry DCM (4.8 mL) was cooled to -78°C . HSiEt_3 (0.49 mL, 3.06 mmol, 2 equiv) and $\text{BF}_3\cdot\text{Et}_2\text{O}$ (0.42 mL, 3.37 mmol, 2.2 equiv) were added sequentially via syringe, and the reaction mixture was stirred for 6 h. The reaction was quenched with sat. NaHCO_3 (4 mL) and warmed to rt. The mixture was diluted with DCM, and the organic phase was separated, washed with sat. NH_4Cl (5 mL), dried over MgSO_4 , and concentrated. The crude product was purified by flash chromatography (heptanes/EtOAc, 2:1) to afford the title compound as a pale yellow oil (334 mg, 69% yield over two steps). ^1H NMR (CDCl_3) δ 6.69–6.64 (m, $J = 4.7, 3.2$ Hz, 2H), 6.61 (dd, $J = 8.0, 1.6$ Hz, 1H), 5.85 (s, 2H), 3.82–3.58 (m, 3H), 3.53 (dd, $J = 11.4, 6.0$ Hz, 1H), 3.26 (ddd, $J = 11.0, 9.4, 6.7$ Hz, 1H), 2.88–2.73 (m, 1H), 2.05 (br s, 1H), 1.89–1.72 (m, 1H), 1.42 (s, 9H). ^{13}C NMR

(CDCl₃) δ (two rotamers) 156.4, 154.4, 147.9, 146.4, 136.7, 134.7, 120.7, 120.4, 108.2, 107.5, 100.9, 80.3, 80.0, 66.9, 66.0, 65.2, 62.4, 47.3, 46.8, 46.4, 32.8, 32.0, 28.3. MS (*m/z*) calcd. for C₁₇H₂₄NO₅ [M + H]⁺ 322.16, found 222.1 [(M + H)-Boc]⁺. [α]₂₅^D -18.3 (*c* = 1.2, MeOH). R_f 0.38 (heptanes/EtOAc, 2:1).

(2*S*,3*R*)-*tert*-Butyl 3-(4-Fluoro-3-(hydroxymethyl)phenyl)-2-(hydroxymethyl)pyrrolidine-1-carboxylate (**6k**). In a flame-dried flask a solution of **4k** (793 mg, 1.40 mmol, 1.0 equiv) in dry THF (4.3 mL) was cooled to -78 °C. LiEtH₃ 1 M (1.68 mL, 1.675 mmol, 1.2 equiv) was added via syringe dropwise, and the reaction mixture was stirred for 1 h, then quenched with sat. NaHCO₃ (5 mL). The aqueous phase was extracted with EtOAc (3 × 10 mL), and the combined organic layers were washed with brine (10 mL), dried over MgSO₄, and concentrated to give the corresponding hemiaminal **5k** as a colorless oil, which was used in the next step without further purification.

In a flame-dried flask a solution of the crude hemiaminal (1.40 mmol, 1.0 equiv) in dry DCM (4.43 mL) was cooled to -78 °C. HSiEt₃ (0.44 mL, 2.79 mmol, 2 equiv) and BF₃·Et₂O (0.38 mL, 3.07 mmol, 2.2 equiv) were added sequentially via syringe, and the reaction mixture stirred for 5 h at -78 °C. The reaction mixture was quenched with sat. NaHCO₃ (5 mL), warmed to rt, and diluted with DCM. The organic phase was separated, washed with sat. NH₄Cl (5 mL), dried over MgSO₄, and concentrated. The crude was dissolved in dry THF under N₂ atmosphere at rt, and 1 M TBAF (THF solution) (1.02 mL, 1.02 mmol, 3 equiv) was added dropwise. The reaction mixture was allowed to stir overnight, quenched with sat. NaHCO₃ (5 mL), and portioned between EtOAc (10 mL) and H₂O (10 mL). The layers were separated, and the aqueous layer was extracted with EtOAc (2 × 10 mL). The combined organic layers were washed with brine (1 × 10 mL), dried over MgSO₄, and concentrated. The crude product was purified by flash chromatography (heptanes/EtOAc, 2:3) to afford the title compound as a colorless oil (92 mg, 20% over three steps). ¹H NMR (CDCl₃, 400 MHz) δ 7.35–7.26 (m, 1H), 7.08 (ddd, *J* = 7.7, 5.0, 2.4 Hz, 1H), 6.95 (dd, *J* = 9.7, 8.4 Hz, 1H), 5.13 (br s, 1H), 4.68 (s, 2H), 3.95–3.53 (m, 4H), 3.31 (td, *J* = 10.4, 6.4 Hz, 1H), 2.90 (br s, 1H), 2.22–2.05 (m, 1H), 1.89 (ddd, *J* = 12.6, 10.5, 8.2 Hz, 1H), 1.47 (s, 9H). ¹³C NMR (CDCl₃, 600 MHz) δ 160.3, 158.6, 156.8, 154.7, 138.3, 136.6, 128.6, 128.5, 128.13, 128.10, 115.5, 115.4, 80.7, 67.1, 66.1, 65.6, 62.8, 58.94, 58.91, 47.2, 47.1, 46.7, 46.5, 33.0, 32.3, 28.5. MS (*m/z*) calcd. for C₁₇H₂₅FNO₄ [M + H]⁺ 326.2, found 226.1 [(M-Boc) + H]⁺. R_f 0.18 (heptanes/EtOAc, 1:1).

(2*S*,3*R*)-*tert*-Butyl 3-(4-Chloro-3-(hydroxymethyl)phenyl)-2-(hydroxymethyl)pyrrolidine-1-carboxylate (**6l**). In a flame-dried flask a solution of **4l** (1.31 g, 2.24 mmol, 1 equiv) in dry THF (6.85 mL) was cooled to -78 °C. LiEtH₃ 1 M (2.69 mL, 2.69 mmol, 1.2 equiv) was added via syringe dropwise, and the reaction mixture was stirred for 1 h, quenched with sat. NaHCO₃ (6 mL), and warmed to rt. The aqueous phase was extracted with EtOAc (3 × 10 mL), and the combined organic layers were washed with brine (10 mL), dried over MgSO₄, and concentrated to give the corresponding hemiaminal **5l** as a colorless oil, which was used in the next step without further purification.

In a flame-dried flask a solution of the crude hemiaminal **5l** (2.24 mmol, 1 equiv) in dry DCM (7.1 mL) was cooled to -78 °C. HSiEt₃ (0.71 mL, 4.476 mmol, 2 equiv) and BF₃·Et₂O (0.62 mL, 4.94 mmol, 2.2 equiv) were sequentially added via syringe, and the reaction mixture was stirred for 5 h at -78 °C. After the complete consumption of the substrate, the reaction was quenched with sat. NaHCO₃ (4 mL) and warmed to rt. The mixture was diluted with DCM, and the organic phase was separated, washed with sat. NH₄Cl (5 mL), dried over MgSO₄, and concentrated to give 1.12 g. The crude product was dissolved in dry THF under N₂ atmosphere at rt, and 1 M TBAF-THF solution (6.7 mL, 6.71 mmol, 3 equiv) was added dropwise. After 2 h, the reaction mixture was quenched with sat. NaHCO₃ (5 mL), EtOAc (10 mL), and H₂O (10 mL). The layers were separated, and the aqueous layer was extracted with EtOAc (2 × 10 mL). The combined organic layers were washed with brine (1 × 10 mL), dried over MgSO₄, and concentrated to dryness. The crude product was purified by flash chromatography (heptanes/EtOAc, 2:1 → 3:2) to

afford the title compounds as a colorless oil (370 mg, 49% over three steps). ¹H NMR (CDCl₃) δ 7.37 (d, *J* = 1.9 Hz, 1H), 7.25 (d, *J* = 8.2 Hz, 1H), 7.04 (dd, *J* = 8.2, 2.2 Hz, 1H), 4.69 (s, 2H), 4.00–3.48 (m, 6H), 3.41–3.24 (m, 1H), 2.92 (s, 1H), 2.12 (dtd, *J* = 9.4, 6.4, 2.9 Hz, 1H), 1.89 (dq, *J* = 12.3, 9.7 Hz, 1H), 1.47 (s, 9H). ¹³C NMR (CDCl₃) δ 156.7, 139.9, 139.0, 130.9, 129.5, 127.5, 127.5, 80.7, 66.8, 65.5, 62.3, 47.2, 47.0, 32.8, 28.5. MS (*m/z*) calcd. for C₁₇H₂₅ClNO₄ [M + H]⁺ 342.1, found 242.1 [(M-Boc) + H]⁺. R_f 0.25 (heptanes/EtOAc, 6:4).

tert-Butyl (2*S*,3*R*)-2-(Hydroxymethyl)-3-(3-(hydroxymethyl)-4-methylphenyl)pyrrolidine-1-carboxylate (**6m**). Compound **4m** (211 mg, 0.037 mmol) was dissolved in dry THF (3.1 mL), and dimethylsulfide borane complex (0.11 mL, 10.5 M in THF) was added dropwise. The reaction mixture was refluxed for 2.5 h, after which it was allowed to cool down to rt and diluted with Et₂O, quenched with sat. NH₄Cl, and the organic portion separated. The organic partition was washed with brine, dried over MgSO₄, filtered through Celite, and concentrated *in vacuo*. The crude product was dissolved in THF (4.7 mL) and treated with TBAF (1 M, 2.24 mL) at rt for 23 h. The mixture was diluted with EtOAc and washed consecutively with NH₄Cl (1 M), H₂O, and brine, and dried over MgSO₄. The solution was concentrated under reduced pressure and purified by flash column chromatography (heptanes/EtOAc, 10:1 → EtOAc) to provide the title compound as a colorless syrup (117 mg, 97%). ¹H NMR (400 MHz, CDCl₃) δ (two rotamers) 7.25 (s, 1H), 7.11–7.07 (m, 1H), 7.06–7.01 (m, 1H), 4.68–4.50 (m, 2H), 3.99–3.84 (m, 1H), 3.72 (m, 2H), 3.65–3.55 (m, 1H), 3.38–3.26 (m, 1H), 2.87 (m, 1H), 2.30–2.25 (m, 3H), 2.15–2.05 (m, 1H), 2.00–1.86 (m, 1H), 1.49 (s, 9H). ¹³C NMR (101 MHz, CDCl₃) δ 156.93, 139.42, 130.66, 128.87, 126.69, 126.45, 114.21, 80.66, 67.02, 65.78, 63.11, 47.56, 47.22, 33.00, 28.57, 18.27. R_f 0.05 (heptanes/EtOAc, 10:1).

(2*S*,3*R*)-1-(*tert*-Butoxycarbonyl)-3-(3-chlorophenyl)pyrrolidine-2-carboxylic Acid (**7d**). A solution of NaIO₄ (434 mg, 2.03 mmol, 4.1 equiv) and RuCl₃·xH₂O (3.1 mg, 0.015 mmol, 0.03 equiv) in H₂O (6.2 mL) was added to a solution of **6d** (154 mg, 0.494 mmol, 1 equiv) in MeCN/EtOAc (1:1, 7.0 mL) cooled to 0 °C. The reaction mixture was stirred for 30 min, then filtered through Celite, and the filter cake was washed with EtOAc. The aqueous layer was extracted with EtOAc, and the combined organic layers were washed with brine, dried over MgSO₄, and concentrated. The crude product was purified by flash chromatography (heptanes/EtOAc, 1:1 + 1% AcOH) to afford the title compound as an off-white solid (138 mg, 86%). ¹H NMR (CDCl₃) δ (two rotamers) 9.64 (br s, 1H), 7.27–7.22 (m, 3H), 7.15–7.13 (m, 1H), 4.40 (d, *J* = 5.5 Hz, 0.4H), 4.25 (d, *J* = 6.5 Hz, 0.6H), 3.79–3.44 (m, 3H), 2.38–2.28 (m, 1H), 2.06–1.96 (m, 1H), 1.49 (s, 4H), 1.42 (s, 5H). ¹³C NMR (CDCl₃) δ (two rotamers) 177.6, 175.7, 155.2, 153.7, 142.9, 142.4, 134.6, 130.1, 127.5, 127.4, 127.1, 125.2, 81.2, 80.1, 65.4, 64.9, 49.4, 47.5, 46.1, 45.9, 32.7, 32.2, 28.3, 28.2. LC-MS (*m/z*) calcd. for C₁₆H₂₁ClNO₄ [M + H]⁺ 326.12, found 226.0 [(M + H)-Boc]⁺. [α]₂₅^D +40.5 (*c* = 0.55, MeOH). R_f 0.27 (heptanes/EtOAc, 1:1 + 1% AcOH). Mp: decomposition.

(2*S*,3*R*)-1-(*tert*-Butoxycarbonyl)-3-(3-(trifluoromethyl)phenyl)pyrrolidine-2-carboxylic Acid (**7e**). A solution of NaIO₄ (380.6 mg, 1.78 mmol, 4.1 equiv) and RuCl₃·xH₂O (2.7 mg, 0.013 mmol, 0.03 equiv) in H₂O (5.45 mL) was added to a solution of **6e** in MeCN/EtOAc (1:1, 6.2 mL) cooled to 0 °C. The reaction mixture was stirred for 30 min, then was filtered through Celite, and the filter cake was washed with EtOAc. The aqueous layer was extracted with EtOAc, and the combined organic layers were washed with brine, dried over MgSO₄, and concentrated to give the title compound as a colorless sticky oil (95 mg, 61%). ¹H NMR (CDCl₃) δ (two rotamers) 9.26 (br s, 1H), 7.55–7.44 (m, 4H), 4.43 (d, *J* = 5.8 Hz, 0.4H), 4.27 (d, *J* = 6.5 Hz, 0.6H), 3.81–3.52 (m, 3H), 2.42–2.31 (m, 1H), 2.10–1.99 (m, 1H), 1.50 (s, 4H), 1.42 (s, 5H). ¹³C NMR (CDCl₃) δ (two rotamers) 177.4, 175.4, 155.3, 153.7, 141.8, 141.3, 131.1 (q, *J* = 33.0 Hz, C-CF₃), 130.4, 130.3, 129.4, 129.3, 124.2, 124.1, 123.9 (q, *J* = 27.2 Hz, CF₃), 123.8, 123.7, 81.3, 81.1, 65.4, 65.0, 49.5, 47.6, 46.1, 45.9, 32.8, 32.3, 28.3, 28.1. [α]₂₅^D +27.9 (*c* = 0.64, MeOH). R_f 0.26 (heptanes/EtOAc, 1:1 + 1% AcOH).

(2*S*,3*R*)-1-(*tert*-Butoxycarbonyl)-3-(3-(*tert*-butoxycarbonyl)-amino)phenyl)pyrrolidine-2-carboxylic Acid (**7f**). A solution of

NaIO₄ (179 mg, 0.836 mmol, 4.1 equiv) and RuCl₃·xH₂O (1.27 mg, 0.006 mmol, 0.03 equiv) in H₂O (2.55 mL) was added to a solution of **6f** (80 mg, 0.204 mmol, 1 equiv) in MeCN/EtOAc (1:1, 2.9 mL) cooled to 0 °C. The reaction mixture was stirred for 30 min, then filtered through filter paper, and the filter cake was washed with EtOAc. The aqueous layer was extracted with EtOAc, and the combined organic layers were washed with brine, dried over MgSO₄, and concentrated to give 128 mg. The crude product was purified by flash chromatography (heptanes/EtOAc, 1:1 + 1% AcOH) to afford the title compound as a colorless oil (41 mg, 49% yield). ¹H NMR (CDCl₃) δ (two rotamers) 10.51 (s, 1H), 7.30 (bs, 1H), 7.25–7.16 (m, 2H), 6.94–6.89 (m, 1H), 6.73 (bs, 1H), 4.41 (d, *J* = 5.4 Hz, 0.4H), 4.25 (d, *J* = 6.5 Hz, 0.6H), 3.85–3.35 (m, 3H), 2.42–2.18 (m, 1H), 2.07–1.96 (m, 1H), 1.51 (s, 9H), 1.49 (s, 4H), 1.41 (s, 5H). ¹³C NMR (CDCl₃) δ (two rotamers) 178.1, 177.1, 175.8, 155.6, 153.9, 142.0, 141.5, 139.0, 138.9, 129.5, 121.7, 117.7, 117.4, 81.3, 80.9, 65.7, 65.3, 60.6, 50.0, 47.8, 46.4, 46.1, 32.9, 32.5, 28.5, 28.5, 28.4. [α]₂₅^D +48.4 (*c* = 0.28, MeOH). *R*_f 0.21 (heptanes/EtOAc, 1:1 + 1% AcOH).

(2*S*,3*R*)-1-(*tert*-Butoxycarbonyl)-3-(3-cyanophenyl)pyrrolidine-2-carboxylic Acid (**7g**). A solution of NaIO₄ (435 mg, 2.03 mmol, 4.1 equiv) and RuCl₃·xH₂O (3.09 mg, 0.015 mmol, 0.03 equiv) in H₂O (6.19 mL) was added to a solution of **6g** (150 mg, 0.496 mmol, 1 equiv) in MeCN/EtOAc (1:1, 7.04 mL) cooled to 0 °C. The reaction mixture was stirred for 1 h, then filtered through filter paper, and the filter cake was washed with EtOAc. The aqueous layer was extracted with EtOAc (3 × 5 mL), and the combined organic layers were washed with brine, dried over MgSO₄, and concentrated. The crude product was purified by flash chromatography (heptanes/EtOAc, 1:2 + 1% AcOH) to afford the title compound as a white solid (119 mg, 76%). ¹H NMR (CDCl₃) δ (two rotamers) 10.56 (bs, 1H), 7.66–7.37 (m, 4H), 4.37 (d, *J* = 5.6 Hz, 0.5H), 4.23 (d, *J* = 6.6 Hz, 0.5H), 3.83–3.40 (m, 3H), 2.36 (dt, *J* = 11.9, 6.5 Hz, 1H), 2.01 (dq, *J* = 12.7, 7.9 Hz, 1H), 1.48 (s, 4H), 1.41 (s, 5H). ¹³C NMR (CDCl₃) δ (two rotamers) 177.3, 175.3, 155.4, 153.7, 142.5, 142.1, 131.8, 131.7, 131.2, 131.1, 130.8, 130.7, 129.9, 118.6, 113.1, 81.7, 81.3, 65.4, 65.1, 49.3, 47.4, 46.2, 46.0, 32.7, 32.3, 28.5, 28.3. MS (*m/z*) calcd. for C₁₇H₂₁N₂O₄ [M + H]⁺ 317.15, found 217.1 [(M + H)-Boc]⁺. Mp: 141.4–143.1 °C. *R*_f 0.26 (heptanes/EtOAc, 1:2 + 1% AcOH).

(2*S*,3*R*)-1-(*tert*-Butoxycarbonyl)-3-(3-carbamoylphenyl)pyrrolidine-2-carboxylic Acid (**7h**). H₂O₂ 30% (w/w) in H₂O (0.089 mL, 0.870 mmol, 6 equiv) was added dropwise to a solution of **7g** (46 mg, 0.145 mmol, 1 equiv) and K₂CO₃ (80 mg, 0.58 mmol, 4 equiv) in EtOH/H₂O (1:1, 1 mL). The reaction mixture was stirred for 3 h at rt, then cautiously acidified with HCl 1 M (until pH ≈ 3) and extracted with EtOAc (3 × 5 mL). The combined organic layers were washed with brine (1 × 15 mL), dried over MgSO₄, and concentrated to give the title compound (32 mg, 66%). ¹H NMR (CDCl₃) δ (two rotamers) 8.61 (br s, 1H), 7.87–7.61 (m, 2H), 7.48–7.30 (m, 2H), 7.12–6.72 (m, 2H), 4.50 (d, *J* = 6.6 Hz, 0.5H), 4.21 (d, *J* = 7.3 Hz, 0.5H), 3.83–3.40 (m, 3H), 2.44–2.17 (m, 1H), 2.12–1.94 (m, 1H), 1.47 (s, 5H), 1.40 (s, 4H). ¹³C NMR (CDCl₃) δ (two rotamers) 176.4, 175.0, 171.0, 170.9, 155.4, 154.0, 141.2, 141.1, 133.6, 133.3, 131.2, 130.7, 129.3, 129.2, 127.3, 126.8, 126.6, 126.5, 81.3, 81.0, 66.1, 65.3, 50.1, 48.5, 46.7, 46.2, 33.4, 32.4, 28.6, 28.4. LC–MS (*m/z*) calcd. for C₁₇H₂₃N₂O₅ [M + H]⁺ 335.16, found 235.1 [(M + H)-Boc]⁺. Mp: 136.9–139.4 °C. *R*_f 0.13 (heptanes/EtOAc, 1:3 + 1% AcOH).

(2*S*,3*R*)-1-(*tert*-butoxycarbonyl)-3-(3-(4,4,5,5-tetramethyl-1,3,2-dioxaborolan-2-yl)phenyl)pyrrolidine-2-carboxylic Acid (**7i**). A solution of NaIO₄ (231 mg, 1.08 mmol, 4.1 equiv) and RuCl₃·xH₂O (1.63 mg, 0.008 mmol, 0.03 equiv) in H₂O (3.27 mL) was added to a solution of **6i** (106 mg, 0.263 mmol, 1.0 equiv) in MeCN/EtOAc (1:1, 3.7 mL) cooled to 0 °C. The reaction mixture was stirred for 30 min, then filtered through filter paper, and the filter cake was washed with EtOAc. The aqueous layer was extracted with EtOAc (3 × 5 mL), and the combined organic layers were washed with brine, dried over MgSO₄, and concentrated to afford the title compound as an off-white solid (72 mg, 66%). ¹H NMR (CDCl₃) δ (two rotamers) 7.77–7.65 (m, 2H), 7.35–7.32 (m, 2H), 4.46 (d, *J* = 5.6 Hz, 0.4H), 4.30 (d, *J* = 6.7 Hz, 0.6H), 3.85–3.42 (m, 3H), 2.43–2.23 (m, 1H), 2.07 (dt, *J* = 16.9, 8.1 Hz, 1H), 1.50 (s, 4H), 1.42 (s, 5H), 1.34 (s, 12H). ¹³C NMR

(CDCl₃) δ (two rotamers) 178.1, 175.5, 155.7, 153.8, 140.2, 139.76, 134.0, 133.8, 133.3, 133.3, 130.2, 129.6, 128.3, 84.0, 81.3, 80.8, 65.8, 65.3, 50.1, 47.8, 46.4, 46.2, 33.3, 32.8, 28.5, 28.4, 25.0. LC–MS (*m/z*) calcd. for C₂₂H₃₃BNO₆ [M + H]⁺ 418.2, found 318.1 [(M + H)-Boc]⁺. Mp: decomposition. *R*_f 0.40 (heptanes/EtOAc, 1:2 + 1% AcOH).

(2*S*,3*R*)-3-(Benzod[1,3]dioxol-5-yl)-1-(*tert*-butoxycarbonyl)-5-oxopyrrolidine-2-carboxylic Acid (**7j**). IBX (340 mg, 1.21 mmol, 2 equiv) was added to a solution of **6j** (195.0 mg, 0.607 mmol, 1 equiv) in DMSO (2.4 mL) at rt. The reaction mixture was allowed to stir until the total consumption of the starting material (3.5 h), then was quenched with sat. NaHCO₃ (3 mL). The aqueous phase was extracted with EtOAc (3 × 5 mL), and the combined organic layers were washed with brine (10 mL), dried over MgSO₄, and concentrated. The crude aldehyde (colorless oil) was used in the next step without further purification.

The crude aldehyde (0.607 mmol, 1 equiv), NaH₂PO₄·2H₂O (284 mg, 1.82 mmol, 3 equiv), and 2-methyl-2-butene (0.32 mL, 3.04 mmol, 5 equiv) were dissolved in *tert*-BuOH/H₂O (3:1, 3 mL). NaClO₂ was then added, and the reaction mixture was stirred for 1.5 h at rt. After the complete consumption of the starting material, the reaction was quenched with pH 7 phosphate buffer (3 mL), and the aqueous phase was extracted with EtOAc (3 × 10 mL). The combined organic layers were washed with brine (10 mL), dried over MgSO₄, and concentrated. The crude product was purified by flash chromatography (heptanes/EtOAc, 2:1 + 1% AcOH) to afford the title compound as an off-white solid (135 mg, 66% over two steps). ¹H NMR (CDCl₃) δ (two rotamers) 7.93 (br s, 1H), 6.72 (m, 3H), 5.94 (s, 2H), 4.33 (d, *J* = 5.3 Hz, 0.4H), 4.18 (d, *J* = 6.6 Hz, 0.6H), 3.80–3.36 (m, 3H), 2.33–2.22 (m, 1H), 2.07–1.88 (m, 1H), 1.50 (s, 4H), 1.42 (s, 5H). ¹³C NMR (CDCl₃) δ (two rotamers) 178.2, 175.1, 155.9, 153.8, 148.2, 146.9, 146.80, 134.8, 134.3, 120.4, 120.3, 108.5, 107.4, 101.2, 81.6, 80.9, 66.0, 65.6, 49.9, 47.4, 46.4, 46.1, 33.1, 32.7, 28.5, 28.4. LC–MS (*m/z*) calcd. for C₁₇H₂₂NO₆ [M + H]⁺ 336.1, found 236.1 [(M + H)-Boc]⁺. [α]₂₅^D +43.8 (*c* = 1.0, MeOH). Mp: 129.5–131.7. *R*_f 0.32 (heptanes/EtOAc, 1:1 + 1% AcOH).

(2*S*,3*R*)-1-(*tert*-Butoxycarbonyl)-3-(3-carboxy-4-fluorophenyl)pyrrolidine-2-carboxylic Acid (**7k**). A solution of NaIO₄ (496 mg, 2.32 mmol, 8.2 equiv) and RuCl₃·xH₂O (3.5 mg, 0.017 mmol, 0.06 equiv) in H₂O (3.51 mL) was added to a solution of **6k** (92 mg, 0.283 mmol, 1 equiv) in MeCN/EtOAc (1:1, 3.98 mL) cooled to 0 °C. The reaction mixture was stirred for 2 h, then was filtered through filter paper, and the filter cake was washed with EtOAc. The aqueous layer was extracted with EtOAc (3 × 10 mL), and the combined organic layers were washed with brine (10 mL), dried over MgSO₄, and concentrated to give 93 mg. The crude was purified by column chromatography (eluent: hept/EtOAc 1/3 + 1% AcOH) to afford the title compound as white needles (89 mg, 89% yield). ¹H NMR (CDCl₃, 400 MHz) δ (two rotamers) 7.91 (dd, *J* = 6.8, 2.5 Hz, 1H), 7.49 (ddd, *J* = 8.6, 4.4, 2.5 Hz, 1H), 7.15 (dt, *J* = 14.4, 7.2 Hz, 1H), 4.39 (d, *J* = 6.4 Hz, 0.5H), 4.22 (d, *J* = 7.3 Hz, 0.5H), 3.88–3.45 (m, 3H), 2.33 (dt, *J* = 12.4, 6.1 Hz, 1H), 2.10–1.99 (m, 1H), 1.51 (s, 5H), 1.43 (s, 4H). ¹³C NMR (MeOD) δ (two rotamers) 177.9, 176.4, 174.4, 168.4, 168.3, 162.7, 162.6, 161.0, 160.9, 156.2, 153.7, 136.7, 136.2, 134.53, 134.47, 134.0, 133.9, 131.8, 131.4, 118.0, 117.90, 117.86, 117.7, 82.2, 81.3, 65.8, 65.6, 49.3, 46.8, 46.6, 46.2, 33.0, 32.7, 28.5, 28.4, 20.7. LC–MS (*m/z*) calcd. for C₁₇H₂₁FNO₆ [M + H]⁺ 354.1, found 254.1 [(M + H)-Boc]⁺. Mp: 168.5–170.6 °C. *R*_f 0.16 (heptanes/EtOAc, 3:1 + 1% AcOH).

(2*S*,3*R*)-1-(*tert*-Butoxycarbonyl)-3-(3-carboxy-4-chlorophenyl)pyrrolidine-2-carboxylic Acid (**7l**). A solution of NaIO₄ (164 mg, 7.68 mmol, 8.2 equiv) and RuCl₃·xH₂O (11.6 mg, 0.056 mmol, 0.06 equiv) in H₂O (11.6 mL) was added to a solution of **6l** (320 mg, 0.936 mmol, 1 equiv) in MeCN/EtOAc (1:1, 13.2 mL) cooled to 0 °C. The reaction mixture was stirred for 2 h, then was filtered through filter paper, and the filter cake was washed with EtOAc. The aqueous layer was extracted with EtOAc (3 × 10 mL), and the combined organic layers were washed with brine (10 mL), dried over MgSO₄, and concentrated. The crude product was purified by column chromatography (heptanes/EtOAc, 1:3 + 1% AcOH) to afford the title compound as a white solid (205 mg, 51% yield). ¹H NMR (CDCl₃)

δ (two rotamers) 7.88 (d, $J = 2.1$ Hz, 1H), 7.46 (dd, $J = 8.1, 4.4$ Hz, 1H), 7.39 (d, $J = 8.3$ Hz, 1H), 6.91 (br s, 2H), 4.40 (d, $J = 6.2$ Hz, 0.5H), 4.24 (d, $J = 7.2$ Hz, 0.5H), 3.85–3.48 (m, 3H), 2.41–2.30 (m, 1H), 2.03 (dt, $J = 9.1, 8.6$ Hz, 1H), 1.51 (s, 5H), 1.44 (s, 4H). ^{13}C NMR (MeOD) δ (two rotamers) 175.7, 175.3, 169.0, 168.9, 156.0, 155.6, 141.7, 141.2, 132.93, 132.87, 132.80, 132.76, 132.7, 132.31, 132.27, 132.2, 131.1, 130.9, 82.0, 81.6, 67.2, 66.6, 50.5, 47.3, 47.1, 33.8, 33.2, 28.7, 28.5. LC–MS (m/z) calcd. for $\text{C}_{17}\text{H}_{21}\text{ClNO}_6$ $[\text{M} + \text{H}]^+$ 370.1, found 270.0 $[(\text{M} + \text{H})\text{-Boc}]^+$. Mp: 184.2–185.6 °C. R_f 0.26 (heptanes/EtOAc, 3:1 + 1% AcOH).

(2*S*,3*R*)-*tert*-Butyl 3-(3-Bromophenyl)-2-(((*tert*-butyldimethylsilyloxy)methyl)pyrrolidine-1-carboxylate (**8b**). In a flame-dried flask a solution of **4b** (803 mg, 1.66 mmol, 1 equiv) in dry THF (5.1 mL) was cooled to -78 °C. LiEtH_3 1 M (THF solution) (1.99 mL, 1.99 mmol, 1.2 equiv) was added via syringe dropwise, and the reaction mixture was stirred for 1 h, quenched with sat. NaHCO_3 (3 mL), and warmed to rt. The aqueous phase was extracted with EtOAc (3 \times 5 mL), and the combined organic layers were washed with brine (10 mL), dried over MgSO_4 , and concentrated to give the corresponding hemiaminal **5b**, which was used in the next step without further purification.

In a flame-dried flask a solution of the crude hemiaminal **5b** (1.66 mmol, 1 equiv) in dry DCM (5.3 mL) was cooled to -78 °C. HSiEt_3 (0.53 mL, 3.31 mmol, 2 equiv) and $\text{BF}_3 \cdot \text{Et}_2\text{O}$ (0.46 mL, 3.65 mmol, 2.2 equiv) were added sequentially via syringe, and the reaction mixture stirred for 4.5 h. The reaction was quenched with sat. NaHCO_3 (4 mL) and warmed to rt. The mixture was diluted with DCM, and the organic phase was separated, washed with sat. NH_4Cl (5 mL), dried over MgSO_4 , and concentrated to dryness to give crude alcohol **6b**.

TBSCl (300 mg, 1.99 mmol, 1.2 equiv) was added to a solution of the crude alcohol **6b** (1.66 mmol, 1 equiv) and imidazole (282 mg, 4.14 mmol, 2.5 equiv) in dry DMF (11.7 mL) under nitrogen at rt. The reaction mixture was stirred overnight, then poured into H_2O . The aqueous layer was extracted with Et_2O (3 \times 10 mL), and the collective organic layers were washed with 1 M HCl (10 mL) and brine (10 mL), dried over MgSO_4 and concentrated to give 839 mg (crude). The crude product was purified by flash chromatography (heptanes/EtOAc, 9:1) to afford the title compound as a colorless oil (572 mg, 73% over three steps). ^1H NMR (CDCl_3 , 400 MHz) δ 7.39–7.32 (m, 2H), 7.16 (dd, $J = 16.8, 9.0$ Hz, 2H), 4.03–3.27 (m, 6H), 2.35–2.19 (m, 1H), 1.96–1.80 (m, 1H), 1.48 (s, 9H), 0.89 (s, 9H), 0.04 (s, 3H), 0.04 (s, 3H). ^{13}C NMR (CDCl_3) δ 154.3, 146.6, 146.2, 130.7, 130.6, 130.6, 130.3, 129.7, 126.1, 126.0, 122.8, 79.8, 79.4, 65.5, 65.4, 63.2, 61.8, 47.0, 46.6, 46.4, 45.5, 32.8, 31.7, 28.7, 26.0, 18.3, -5.3 . R_f 0.27 (heptanes/EtOAc, 9:1).

(2*S*,3*R*)-*tert*-Butyl 2-(((*tert*-butyldimethylsilyloxy)methyl)-3-(3-cyanophenyl)pyrrolidine-1-carboxylate (**8g**). Aryl bromide **8b** (500 mg, 1.06 mmol, 1 equiv), $\text{Zn}(\text{CN})_2$ (75 mg, 0.64 mmol, 0.6 equiv), Zn powder (8.3 mg, 0.127 mmol, 0.12 equiv), $\text{Pd}_2(\text{dba})_3$ (48.6 mg, 0.053 mmol, 0.05 equiv), and dppf (58.9 mg, 0.106 mmol, 0.1 equiv) were placed in a 10 mL oven-dried flask, which was evacuated and backfilled with N_2 . Dry dimethylacetamide (2.1 mL) was added, and the reaction mixture was stirred at 120 °C for 75 min, then cooled to rt and diluted with EtOAc (5 mL). The organic phase was washed with sat. NaHCO_3 , brine, dried over MgSO_4 , and concentrated. The crude product was purified by column chromatography (heptanes/EtOAc, 95:5) to give the title compound a colorless oil. ^1H NMR (CDCl_3) δ 7.53–7.35 (m, 4H), 3.99–3.58 (m, 4H), 3.57–3.49 (m, 1H), 3.42–3.29 (m, 1H), 2.30 (dtd, $J = 12.8, 7.3, 5.6$ Hz, 1H), 1.87 (dq, $J = 14.3, 7.2$ Hz, 1H), 1.47 (s, 9H), 0.86 (s, 9H), 0.03 (s, 3H), 0.02 (s, 3H). ^{13}C NMR (CDCl_3) δ 154.1, 145.5, 145.3, 131.9, 131.7, 131.0, 130.2, 129.5, 118.8, 112.7, 79.9, 79.5, 65.2, 63.2, 61.8, 46.7, 46.6, 46.1, 45.4, 32.5, 31.6, 28.6, 25.8, 18.2, -5.4 . LC–MS (m/z) calcd. for $\text{C}_{18}\text{H}_{29}\text{N}_2\text{O}_5\text{Si}$ $[(\text{M} + \text{H})\text{-Boc}]^+$ 317.2, found 317.2. R_f 0.59 (heptanes/EtOAc, 2:1).

(2*S*,3*R*)-*tert*-Butyl 2-(((*tert*-butyldimethylsilyloxy)methyl)-3-(3-(4,4,5,5-tetramethyl-1,3,2-dioxaborolan-2-yl)phenyl)pyrrolidine-1-carboxylate (**8i**). (BPin) $_2$ (380 mg, 1.50 mmol, 1.1 equiv), $\text{PdCl}_2(\text{dppf})$ (49.7 mg, 0.068 mmol, 0.05 equiv), and KOAc (400 mg, 4.08 mmol, 3.0 equiv) were placed in an oven-dried flask, which

was evacuated and backfilled with nitrogen. A solution of aryl bromide **8** (640 mg, 1.36 mmol, 1.0 equiv) in dry DMF (8.2 mL) was added via syringe, and the reaction mixture was stirred at 80 °C for 5 h. The reaction mixture was cooled to rt and diluted with H_2O (10 mL). The aqueous layer was extracted with Et_2O (3 \times 10 mL), and the combined organic layers were washed with HCl 1 M (1 \times 10 mL), brine (1 \times 10 mL), dried over MgSO_4 , and concentrated. The crude product was purified by column chromatography (heptanes/EtOAc, 95:5) to give the title compound as a colorless oil (431 mg, 61%). ^1H NMR (CDCl_3) δ 7.71–7.64 (m, 2H), 7.36–7.27 (m, 2H), 4.10–3.49 (m, 5H), 3.43–3.23 (m, 1H), 2.31–2.19 (m, 1H), 1.99–1.88 (m, 1H), 1.49 (s, 9H), 1.34 (s, 12H), 0.89 (s, 9H), 0.04 (s, 6H). ^{13}C NMR (CDCl_3) δ (two rotamers) 154.4, 154.3, 143.2, 142.7, 133.9, 133.7, 133.0, 130.5, 130.3, 129.4 (bs), 128.2, 83.9, 79.5, 79.1, 65.5, 65.4, 63.0, 61.5, 47.2, 46.7, 46.5, 45.7, 33.0, 31.8, 28.7, 26.0, 25.0, 25.0, 18.3, -5.3 . LC–MS (m/z) calcd. for $\text{C}_{28}\text{H}_{49}\text{BNO}_5\text{Si}$ $[\text{M} + \text{H}]^+$ 518.3, found 336.2 $[(\text{M} + \text{H})\text{-Boc-Pin}]^+$. R_f 0.16 (heptanes/EtOAc, 95:5).

Pharmacological Studies. All reagents and solvents were commercial and of high purity analytical grade or ultragradient HPLC-grade purchased from Sigma, (St. Louis, MO, USA), J.T. Baker (Denver, The Netherlands), Merck (Darmstadt, Germany), or Riedel-de Haën (Seelze, Germany). Water was purified using a Milli-Q Gradient system (Millipore, Milford, MA, USA). LPS from *Escherichia coli* 055:B5 and fluorescein were purchased from Sigma (St. Louis, MO, USA). $[\text{^3H}]\text{-digoxin}$, 250 μCi (9.25 MBq), and Emulsifier safe liquid scintillation cocktail were purchased from PerkinElmer (Boston, MA, USA). Prostaglandin E2 was purchased from Biotechne Ltd. (Abingdon, UK) and sorafenib from Cayman Chemical (Ann Arbor, MI, USA).

Liquid Chromatographic and Mass Spectrometric (LC–MS/MS) Analyses. An Agilent 1200 Series Rapid Resolution LC System was used together with a Poroshell 120 EC-C-18 column (50 mm \times 2.1 mm, 2.7 μm) for liquid chromatography prior to MS analysis of compound **11**, sorafenib, and PGE_2 with Agilent 6410 triple quadrupole mass spectrometer equipped with an electrospray ionization source (Agilent Technologies Inc., Wilmington, DE). The high-performance liquid chromatography eluents were water (A) containing 0.1% (v/v) formic acid and acetonitrile (B). For the compound **11**, a gradient elution with 5–60% B was applied over 1–3 min, followed by 1 min of isocratic elution with 60% B and 3 min column equilibration, giving a total time of 7 min/injection. For sorafenib, a gradient elution with 20–90% B was applied over 1–4 min, followed by 1 min of isocratic elution with 90% B and 3 min column equilibration, giving a total time of 8 min/injection. For PGE_2 an isocratic method with 10% B was used. For all compounds the eluent flow rate was 0.2 mL/min, the column temperature was 40 °C, and injection volume was 5 μL . The following mass spectrometry conditions were used for the compound **11**, sorafenib, and PGE_2 . Electrospray ionization: positive ion mode for compound **11**, sorafenib and negative ion mode for PGE_2 ; drying gas (nitrogen) temperature, 300 °C; drying gas flow rate, 8 L/min; nebulizer pressure, 20 psi; and capillary voltage, 3500 V. Analyte detection was performed using multiple reaction monitoring, the transitions being 270.1 \rightarrow 114.5 and 236.1 \rightarrow 190 for compound **11** and **1a** (internal standard), respectively. The transitions for sorafenib and the used internal standard, diclofenac, were 465.1 \rightarrow 252.2 and 296.1 \rightarrow 250, respectively. The transition for PGE_2 was 315.4 \rightarrow 314.5. Fragmentor voltages used for compound **11**, **1a**, sorafenib, diclofenac, and PGE_2 were 60, 140, 140, 100, and 180 V, and the collision energies were 40, 16, 30, 10, and 6 V, respectively. Agilent MassHunter Workstation Acquisition software (Data Acquisition for Triple Quadrupole Mass Spectrometer, version B.03.01) was used for data acquisition, and Quantitative Analysis (B.04.00) software was used for the data processing and analysis. The compound **11** lower limit of quantification for the brain, liver, and plasma samples were 0.02 nmol/g, 0.02 nmol/g, and 0.5 μM respectively. The lower limit of quantification for sorafenib and PGE_2 in cell samples was 1 nM. Linearity of the calibration curves was evaluated by a quadratic regression analysis. The method was also selective, accurate, and precise over the calibration range. Within-run accuracy and precision were calculated from the results of the quality

Table 5. Probe Peptides and MRM Transitions for the LC–MS/MS Analysis of Investigated Transporters

transporter	St/Is	probe peptide sequence	MRM transitions (<i>m/z</i>)			
			Q1	Q3.1	Q3.2	Q3.3
Abcb1	St	NTTGALTR	467.8	618.4	719.4	516.3
	Is	NTTGALTR ^a	472.6	628.4	729.4	571.3
Abcg2	St	SLLLDVLAAR	522.8	757.5	644.3	529.3
	Is	SLLLDVLAAR ^a	527.8	767.5	654.4	539.4
Abcc2	St	LTIIPQDPILFSGNLR	899.0	1356.7	678.9	
	Is	LTIIPQDPILFSGNLR ^a	904.0	1366.7	683.9	
Abcc4	St	APVLFDFR	482.8	796.4	697.4	584.3
	Is	APVLFDFR ^a	487.8	806.4	707.4	594.3
Slc7a5	St	VQDAFAAAK	460.8	693.4	578.3	
	Is	VQDAFAAAK ^a	464.8	701.4	586.3	
Slc2a1	St	TFDEIASGFR	571.8	894.4	537.3	
	Is	TFDEIASGFR ^a	576.8	904.4	547.3	

^aDenotes ¹³C-labeled arginine and lysine.

control samples at the three concentrations. The accuracies and precisions for quality control concentrations of 20% were considered to be acceptable.

Preparation of Crude Membrane Fractions of Mouse HCC Cells. Mouse *Nras* driven *p53*^{-/-} HCC cells were cultured in Dulbecco's modified Eagle's medium (DMEM) supplemented with L-glutamine (2 mM), heat-inactivated fetal bovine serum (10%), penicillin (50 U/mL), and streptomycin (50 μg/mL). The cells were incubated for 48 h with or without 10 μM of compound **11**, washed three times with HBSS, followed by centrifugation of the cells into a pellet and rapid freezing in liquid nitrogen. ProteoExtract Subcellular Proteome Extraction Kit (Merck KGaA, Darmstadt, Germany) was used for the isolation of crude membrane fraction from the cell pellets following the manufacturer's instructions. The protein concentrations in the crude membrane fractions were determined as mean of three samples by Bio-Rad Protein Assay (EnVision, PerkinElmer, Inc., Waltham, MA, USA), and aliquots containing 50 μg of total protein were taken for further sample preparation.

Protein Quantification by Multiplexed Selected/Multiple Reaction Monitoring by LC–MS/MS. The protein expressions of the investigated transporters were simultaneously determined by means of multiplexed multiple reaction monitoring analysis. The aliquots containing 50 μg of protein from the crude membrane fractions were solubilized in 500 mM Tris–HCl (pH 8.5), 7 M guanidine hydrochloride, and 10 mM EDTA, and the proteins were S-carbamoylmethylated with iodoacetamide following dithiothreitol treatment. The alkylated proteins were precipitated using methanol and chloroform. The precipitates were dissolved in 6 M urea in 100 mM Tris–HCl (pH 8.5), diluted five-fold with 100 mM Tris–HCl (pH 8.5), spiked with internal standard peptides, and treated with Protease-Max surfactant (Promega, Madison, WI, USA). The dilutions were treated with lysyl endopeptidase (Lys-C: Wako Pure Chemical Industries, Osaka, Japan) at rt for 3 h, after which tosylphenylalanyl chloromethyl ketone-treated trypsin (Promega, Madison, WI, USA) at an enzyme/substrate ratio of 1:100 was added into the samples and incubated at 37 °C for 16 h. The tryptic digests were mixed formic acid and then centrifuged at 4 °C and 14 000g for 5 min. The supernatant was mixed with water prior to LC–MS/MS analysis.

LC–MS/MS analysis was performed by coupling an Agilent 1290 Infinity LC (Agilent Technologies, Waldbronn, Germany) instrumentation to an Agilent 6495 Triple Quadrupole Mass Spectrometer with an electrospray ionization (ESI) source (Agilent Technologies, Palo Alto, CA, USA) using multiple reaction monitoring (MRM). The following conditions were applied: positive ionization mode, the drying gas (nitrogen) was maintained at 210 °C, drying gas flow rate was 16 L/min, nebulizer gas pressure was 45 psi, sheath gas temperature 300 °C, sheath gas flow 11 L/min, fragmentor voltage was 380 V, and the mass-spectrometer (MS) capillary voltage was 3.0 kV. The following ion funnel parameters were used for both positive

and negative ionization: high-pressure ion funnel RF voltage 200 V, and low-pressure ion funnel RF voltage 100 V. An injection volume of 15 μL was used, and analytes were separated by AdvanceBio Peptide Map 2.1 × 250 mm, 2.7 μm. Mobile phases A and B, respectively, consisted of 0.1% formic acid in milli-Q water and acetonitrile. The gradient sequence was as follows: flow rate of 0.30 mL/min, 50 min of total run time, 97:3 to 60:40 (A:B) during 40 min after injection, 5:95 at 44 min, 97:3 at 45 min, and constant 97:3 for 5 min. The eluted peptides were selectively and simultaneously analyzed by SRM/MRM mode with LC–MS/MS. For each target protein, one unique peptide was chosen according to previously published work.³⁶ These peptides were monitored with two or three different SRM/MRM transition sets (Table 5) derived from one set of stable isotope-labeled peptides purchased from JPT Peptide Technologies GmbH (Berlin, Germany) and unlabeled peptides.

Ability of Compound **11 To Alter the Cell Accumulation of Transporter Probes and Sorafenib.** The ability of compound **11** to increase the cell accumulation of Abcb1 probe [³H]-digoxin, Abcc1–5 probe fluorescein, and Abcb1 and Abcg2 substrate sorafenib as well as to decrease cell accumulation of Slc7a5 probe [¹⁴C]-L-leucine and Slc2a1 probe [¹⁴C]-D-glucose was determined in mouse *Nras* driven *p53*^{-/-} HCC cells. The cells were cultured in DMEM supplemented with L-glutamine (2 mM), heat-inactivated fetal bovine serum (10%), penicillin (50 U/mL), and streptomycin (50 μg/mL). HCC cells were seeded at the density of 1 × 10⁵ cells/well onto 24-well plates. After seeding, the cells were incubated for 24 h with or without 10 μM of compound **11**. In order to ensure that compound **11** does not inhibit the function of the efflux transporters, the incubation medium was removed and the cells were carefully washed three times with prewarmed Hank's balance salt solution (HBSS) containing 125 mM choline chloride, 4.8 mM KCl, 1.2 mM MgSO₄, 1.2 mM KH₂PO₄, 1.3 mM CaCl₂, 5.6 mM glucose, 100 μM leucine, and 25 mM HEPES (pH 7.4), after which a transporter probe, [³H]-digoxin, [¹⁴C]-L-leucine, [¹⁴C]-D-glucose, 20 μM fluorescein, or 10 μM sorafenib, was added in prewarmed HBSS buffer (250 μL) on the top of the cell layer and incubating at 37 °C for 30 min for [³H]-digoxin, fluorescein and sorafenib or 5 min for [¹⁴C]-L-leucine and [¹⁴C]-D-glucose. Subsequently, the cells were washed three times with ice-cold HBSS and lysed with 500 μL of 0.1 M NaOH. The protein concentrations in each well were determined by Bio-Rad Protein Assay (EnVision, PerkinElmer, Inc., Waltham, MA, USA). The lysate from the [³H]-digoxin, [¹⁴C]-L-leucine, and [¹⁴C]-D-glucose samples was mixed with 3.5 mL of emulsifier safe liquid scintillation cocktail. The radioactivity was measured by liquid scintillation counting (Wallac 1450 MicroBeta; Wallac Oy, Finland). The fluorescein samples were measured using fluorescein detector (EnVision, PerkinElmer, Inc., Waltham, MA, USA), and the sorafenib concentrations were determined by the LC–MS/MS.

Live Imaging of Murine HCC Cell Culture. The cells were loaded with the Ca²⁺ sensitive fluorescent dye Fluo-4-AM (5 μM) for

45 min followed by a 20 min washout in the BSS containing the following (in millimolar): 2.5 KCl, 152 NaCl, 10 glucose, 2 CaCl₂, and 10 HEPES at pH 7.4. Fluorescence was visualized using the imaging setup (TILL Photonics GmbH) consisting of a monochromatic light source and a CCD camera (SensiCam). Cells loaded with Fluo-4 were imaged with an excitation light of 495 nm (exposure time 100 ms, binning 2). Chemicals were applied using a fast perfusion system (Rapid Solution Changer RSC-200, BioLogic Science). Data were analyzed offline using the TILL Photonics and Origin 8 software.

Ability of 11 To Decrease PGE₂ Concentration in the Cells.

The ability of compound 11 to decrease PGE₂ synthesis was studied in HCC cells with and without LPS-induced inflammation. The LPS concentration in the growth medium was 2.5 μg/mL. The cells were incubated 24 h with or without 100 μM compound 11. Subsequently, the cells were washed three times with ice-cold HBSS, and then lysed with 500 μL of acetonitrile on ice. The PGE₂ concentrations from the cell lysates were determined by the LC-MS/MS.

Antiproliferative Activity in Vitro. The mouse HCC cells were seeded at the density of 2×10^4 cells/well onto collagen-coated 96-well plates, and the cells were used for the experiments 1 day after seeding. A concentration of 1, 2.5, 5, and 10 μM sorafenib, 100 μM compound 11, and the combination of all the mentioned sorafenib concentrations with 100 μM compound 11 were added into the growth medium and incubated for 3 days. Each day the medium was changed, and after the 72 h incubation, the cell viability was determined by resazurin cell proliferation kit (Sigma, St. Louis, MO, USA), which is directly proportional to aerobic respiration and cellular metabolism of cells. The samples were measured fluorometrically by monitoring the increase in fluorescence at a wavelength of 590 nm using an excitation wavelength of 560 nm (EnVision, PerkinElmer, Inc., Waltham, MA, USA). The cell death was confirmed in the decrease of cell amount by visualizing the wells with microscopy.

Animals. Adult male mice weighing 25 ± 5 g were supplied by the National Laboratory Animal Centre (Kuopio, Finland). Mice were housed in stainless steel cages on a 12 h light (07:00–19:00) and 12 h dark (19:00–07:00) cycle at an ambient temperature of 22 ± 1 °C with a relative humidity of 50–60%. All experiments were carried out during the light phase. Tap water and food pellets (Lactamin R36; Lactamin AB, Södertälje, Sweden) were available ad libitum. All procedures with the animals were performed according to European Community Guidelines and Guide for the Care and Use of Laboratory Animals (National Institutes of Health publication no. 85–23, revised in 1985). The procedures were reviewed and approved by the Finnish National Animal Experiment Board.

In Situ Mouse Brain Perfusion. Mice were anesthetized with intraperitoneal (i.p.) injections of ketamine (120 mg/kg) and xylazine (8 mg/mL), and their right carotid artery system was exposed. The right external carotid artery was ligated, and the right common carotid artery was cannulated with a catheter filled with 100 IU/mL heparin. The perfusions were performed at 37 °C with a flow rate of 2.5 mL/min for 60 s followed by the washing of the capillaries for 2 s with 4 °C drug-free perfusion buffer. The method is described in more detail by Gynther et al.³⁷

In Vivo Pharmacokinetics of Compound 11. A 5.0 mM concentration of compound 11 was dissolved in a vehicle containing 0.9% (w/v) NaCl in water. A dose of 10 mg/kg of compound 11 was administered as a bolus injection (i.p.) to mice. The mice were sacrificed by decapitation at selected time points between (10–240 min), and plasma, brain, and liver were collected for analysis.

Plasma and Tissue Sample Preparation. Plasma samples were prepared by precipitating 100 μL of plasma with 200 μL of acetonitrile containing the internal standard (1a). Samples were vortexed and centrifuged for 10 min at 14 000g at 4 °C. Then 100 μL of supernatant was mixed with 100 μL of ultrapure water prior to LC-MS/MS analysis. Tissue samples were weighed and homogenized with ultrapure water (1:3). An aliquot of 100 μL was taken, and the analyte was isolated from the samples by protein precipitation with 300 μL of acetonitrile containing the internal standard. Samples were vortexed and centrifuged for 10 min at 14 000g at 4 °C. Then 200 μL

of supernatant was mixed with 100 μL of ultrapure water prior to LC-MS/MS analysis.

Two-Electrode Voltage-Clamp Electrophysiology. Rat cDNAs encoding GluN1–1a (Genbank accession number U11418 and U08261; hereafter GluN1), GluN2A (D13211), GluN2B (U11419), GluN2C (M91563), and GluN2D (L31611) were generously provided by Dr. S. Heinemann (Salk Institute, La Jolla, CA), Dr. S. Nakanishi (Osaka Bioscience Institute, Osaka, Japan), and Dr. P. Seeburg (University of Heidelberg). The cDNA encoding rat GluN2B was modified without changing the amino acid sequence to remove a T7 RNA polymerase termination site located in the C-terminal domain.³⁸

For expression in *Xenopus laevis* oocytes, cDNAs were linearized using restriction enzymes and used as templates to synthesize cRNA using the mMessage mMachine kit (Ambion, Life Technologies, Paisley, UK). *Xenopus* oocytes were obtained from Rob Weymouth (*Xenopus* 1, Dexter, MI) and prepared as previously described.³⁹ The oocytes were injected with cRNAs encoding GluN1 and GluN2 in a 1:2 ratio and maintained at 18 °C in Barth's solution containing 88 mM NaCl, 1 mM KCl, 2.4 mM NaHCO₃, 0.82 mM MgSO₄, 0.33 mM Ca(NO₃)₂, 0.91 mM CaCl₂, 10 mM HEPES (pH 7.5 with NaOH) supplemented with 100 IU/mL penicillin, 100 μg/mL streptomycin, and 50 μg/mL gentamycin (Invitrogen, Life Technologies, Paisley, UK). Two-electrode voltage-clamp recordings were performed on *Xenopus* oocytes at rt 2–6 days postinjection with the extracellular recording solution comprising 90 mM NaCl, 1 mM KCl, 10 mM HEPES, 0.5 mM BaCl₂, and 0.01 mM EDTA (pH 7.4 with NaOH) at a holding potential of –40 mV essentially as previously described.³⁹ NMDA receptor ligands were dissolved in extracellular recording solution and applied to the oocyte by gravity-driven perfusion.

Data Analysis. All statistical analyses were performed using GraphPad Prism v. 5.03 software (GraphPad Software, San Diego, CA, USA). Statistical differences between groups were tested using two-tailed *t* test (Figures 1 and 2). Concentration–inhibition data were measured using two-electrode voltage-clamp electrophysiology fitted to the Hill equation to obtain IC₅₀ values for individual oocytes as previously described.³⁹ The sorafenib IC₅₀ value for cytotoxicity in murine HCC cells was calculated by nonlinear regression analysis and presented as the mean ± SEM. The pharmacokinetic parameters, AUC_{0–240 min}, C_{max}, t_{max}, and t_{1/2β} in plasma, brain, and liver, were obtained from the pharmacokinetic data.

Radioligand Binding. Ligand affinities at native AMPA, KA, and NMDA receptors (rat brain synaptosomes) were determined using [³H]AMPA, [³H]KA, and [³H]CGP-39653, respectively, as previously described.⁴⁰ Ligand affinities at recombinant homomeric rat GluK1–3 were determined using [³H]KA as the radioligand as previously detailed (Sagot et al. and Alcaide et al.).^{41,42} Data were analyzed using GraphPad Prism 7 (GraphPad Software, San Diego, CA) to determine ligand IC₅₀ and K_i values.

In Silico Studies. Calculation of LogP(o/w) and total polar surface area (TPSA) was done in MOE version 2016.08.02 released by Chemcomp corporation.

■ ASSOCIATED CONTENT

Supporting Information

The Supporting Information is available free of charge on the ACS Publications website at DOI: 10.1021/acs.jmedchem.7b01624.

SMILES (CSV)

■ AUTHOR INFORMATION

Corresponding Authors

*E-mail: lebu@sund.ku.dk. Phone: +45 35 33 62 44.

*E-mail: mikko.gynther@uef.fi.

ORCID

Kasper B. Hansen: 0000-0002-3303-4819

Darryl S. Pickering: 0000-0001-8687-6094

Lennart Bunch: 0000-0002-0180-4639

Author Contributions

[†]These authors contributed equally to this work.

Notes

The authors declare no competing financial interest.

ACKNOWLEDGMENTS

We would like to thank the Lundbeck Foundation and the Danish Medical Research Council for financial support of the medicinal chemistry work reported herein. Emil Aaltonen Foundation and The Finnish Cultural Foundation are acknowledged for the funding regarding the pharmacokinetic analysis, transporter expression modulation, and cytotoxicity studies. Finally, the National Institutes of Health (P20GM103546 and R01NS097536) is acknowledged for financial support in regards to the functional characterization of **11** at NMDA receptors. Mrs. Sari Ukkonen is acknowledged for technical assistance. The murine hcc cells were a kind donation by Prof. Lars Zender, Tübingen University.

ABBREVIATIONS USED

ABC, ATP-binding cassette; Abcb1, ATP-binding cassette subfamily B member 1; Abcc, ATP-binding cassette subfamily C; Abcg2, ATP-binding cassette subfamily G member 2; AUC, area under the concentration curve; BBB, blood–brain barrier; C_{max} , maximum concentration; cPLA2, cytoplasmic phospholipase A2; DCM, dichloromethane; DCVC, dry collum vacuum chromatography; DMAP, *N,N*-dimethyl-4-aminopyridine; DMEM, Dulbecco's modified Eagle medium; DMF, *N,N*-dimethylformamide; DMSO, *N,N*-dimethylsulfonamide; HBSS, Hank's balance salt solution; HCC, hepatocellular carcinoma; IBX, 2-iodoxybenzoic acid; LC–MS/MS, liquid chromatography–mass spectrometry; LPS, lipopolysaccharide; MDR, multidrug resistance; MRM, multiple reaction monitoring; PGE₂, prostaglandin E2; SRM, selected reaction monitoring; TBAF, tetrabutylammonium fluoride; TBSCl, *tert*-butyldimethylsilyl chloride; TFA, trifluoroacetic acid; T_{max} , time to reach the maximum concentration; $t_{1/2\beta}$, elimination half-life

REFERENCES

- (1) Holohan, C.; Van Schaeybroeck, S.; Longley, D. B.; Johnston, P. G. Cancer Drug Resistance: An Evolving Paradigm. *Nat. Rev. Cancer* **2013**, *13*, 714–726.
- (2) Rudalska, R.; Dauch, D.; Longerich, T.; McJunkin, K.; Wuestefeld, T.; Kang, T.-W. T.-W. T.-W.; Hohmeyer, A.; Pesic, M.; Leibold, J.; von Thun, A.; Schirmacher, P.; Zuber, J.; Weiss, K.-H. K.-H.; Powers, S.; Malek, N. P. N. P.; Eilers, M.; Sipos, B.; Lowe, S. W. S. W. S. W.; Geffers, R.; Laufer, S.; Zender, L. In Vivo RNAi Screening Identifies a Mechanism of Sorafenib Resistance in Liver Cancer. *Nat. Med.* **2014**, *20*, 1138–1146.
- (3) Szakács, G.; Paterson, J. K.; Ludwig, J. A.; Booth-Genthe, C.; Gottesman, M. M. Targeting Multidrug Resistance in Cancer. *Nat. Rev. Drug Discovery* **2006**, *5*, 219–234.
- (4) Zhang, Y.-K.; Wang, Y.-J.; Gupta, P.; Chen, Z.-S. Multidrug Resistance Proteins (MRPs) and Cancer Therapy. *AAPS J.* **2015**, *17*, 802–812.
- (5) Stacy, A. E.; Jansson, P. J.; Richardson, D. R. Molecular Pharmacology of ABCG2 and Its Role in Chemoresistance. *Mol. Pharmacol.* **2013**, *84*, 655–669.
- (6) Gillet, J.-P.; Efferth, T.; Remacle, J. Chemotherapy-Induced Resistance by ATP-Binding Cassette Transporter Genes. *Biochim. Biophys. Acta, Rev. Cancer* **2007**, *1775*, 237–262.
- (7) Wu, C. P.; Hsieh, C. H.; Wu, Y. S. The Emergence of Drug Transporter-Mediated Multidrug Resistance to Cancer Chemotherapy. *Mol. Pharmaceutics* **2011**, *8*, 1996–2011.
- (8) Rigalli, J. P.; Ciriaci, N.; Arias, A.; Ceballos, M. P.; Villanueva, S. S. M.; Luquita, M. G.; Mottino, A. D.; Ghanem, C. I.; Catania, V. A.; Ruiz, M. L. Regulation of Multidrug Resistance Proteins by Genistein in a Hepatocarcinoma Cell Line: Impact on Sorafenib Cytotoxicity. *PLoS One* **2015**, *10*, e0119502.
- (9) Huang, W. C.; Hsieh, Y. L.; Hung, C. M.; Chien, P. H.; Chien, Y. F.; Chen, L. C.; Tu, C. Y.; Chen, C. H.; Hsu, S. C.; Lin, Y. M.; Chen, Y. J. BCRP/ABCG2 Inhibition Sensitizes Hepatocellular Carcinoma Cells to Sorafenib. *PLoS One* **2013**, *8*, e83627.
- (10) Gnoth, M. J.; Sandmann, S.; Engel, K.; Radtke, M. In Vitro to In Vivo Comparison of the Substrate Characteristics of Sorafenib Tosylate toward P-Glycoprotein. *Drug Metab. Dispos.* **2010**, *38*, 1341–1346.
- (11) Callaghan, R.; Luk, F.; Bebawy, M. Inhibition of the Multidrug Resistance P-Glycoprotein: Time for a Change of Strategy? *Drug Metab. Dispos.* **2014**, *42*, 623–631.
- (12) Fletcher, J. I.; Haber, M.; Henderson, M. J.; Norris, M. D. ABC Transporters in Cancer: More than Just Drug Efflux Pumps. *Nat. Rev. Cancer* **2010**, *10*, 147–156.
- (13) Traynelis, S. F.; Wollmuth, L. P.; McBain, C. J.; Menniti, F. S.; Vance, K. M.; Ogden, K. K.; Hansen, K. B.; Yuan, H.; Myers, S. J.; Dingledine, R. Glutamate Receptor Ion Channels: Structure, Regulation, and Function. *Pharmacol. Rev.* **2010**, *62*, 405–496.
- (14) Qosa, H.; Miller, D. S.; Pasinelli, P.; Trotti, D. Regulation of ABC Efflux Transporters at Blood-Brain Barrier in Health and Neurological Disorders. *Brain Res.* **2015**, *1628*, 298–316.
- (15) Leslie, C. C. Properties and Regulation of Cytosolic Phospholipase A2. *J. Biol. Chem.* **1997**, *272*, 16709–16712.
- (16) Maeda, S.; Omata, M. Inflammation and Cancer: Role of Nuclear Factor- κ B Activation. *Cancer Sci.* **2008**, *99*, 836–842.
- (17) Shi, Y.; Wang, S.-Y.; Yao, M.; Sai, W.-L.; Wu, W.; Yang, J.-L.; Cai, Y.; Zheng, W.-J.; Yao, D.-F. Chemosensitization of HepG2 Cells by Suppression of NF- κ B/p65 Gene Transcription with Specific-siRNA. *World J. Gastroenterol.* **2015**, *21*, 12814–12821.
- (18) Deutsch, S. I.; Tang, A. H.; Burket, J. A.; Benson, A. D. NMDA Receptors on the Surface of Cancer Cells: Target for Chemotherapy? *Biomed. Pharmacother.* **2014**, *68*, 493–496.
- (19) Ribeiro, M. P. C.; Nunes-Correia, I.; Santos, A. E.; Custódio, J. B. A. The Combination of Glutamate Receptor Antagonist MK-801 with Tamoxifen and Its Active Metabolites Potentiates Their Antiproliferative Activity in Mouse Melanoma K1735-M2 Cells. *Exp. Cell Res.* **2014**, *321*, 288–296.
- (20) Yamaguchi, F.; Hirata, Y.; Akram, H.; Kamitori, K.; Dong, Y.; Sui, L.; Tokuda, M. FOXO/TXNIP Pathway Is Involved in the Suppression of Hepatocellular Carcinoma Growth by Glutamate Antagonist MK-801. *BMC Cancer* **2013**, *13*, 468.
- (21) Bergeron, R.; Coyle, J. T. NAAG, NMDA Receptor and Psychosis. *Curr. Med. Chem.* **2012**, *19*, 1360–1364.
- (22) Ghose, A. K.; Viswanadhan, V. N.; Wendoloski, J. J. A Knowledge-Based Approach in Designing Combinatorial or Medicinal Chemistry Libraries for Drug Discovery. I. A Qualitative and Quantitative Characterization of Known Drug Databases. *J. Comb. Chem.* **1999**, *1*, 55–68.
- (23) Larsen, A. M.; Venskutonytė, R.; Valadés, E. A.; Nielsen, B.; Pickering, D. S.; Bunch, L. Discovery of a New Class of Iontropic Glutamate Receptor Antagonists by the Rational Design of (2S,3R)-3-(3-Carboxyphenyl)-Pyrrolidine-2-Carboxylic Acid. *ACS Chem. Neurosci.* **2011**, *2*, 107–114.
- (24) Krogsgaard-Larsen, N.; Storgaard, M.; Møller, C.; Demmer, C. S.; Hansen, J.; Han, L.; Monrad, R. N.; Nielsen, B.; Tapken, D.; Pickering, D. S.; Kastrup, J. S.; Frydenvang, K.; Bunch, L. Structure-Activity Relationship Study of Iontropic Glutamate Receptor Antagonist (2S,3R)-3-(3-Carboxyphenyl)pyrrolidine-2-Carboxylic Acid. *J. Med. Chem.* **2015**, *58*, 6131–6150.
- (25) Ogura, A.; Yamada, K.; Yokoshima, S.; Fukuyama, T. Total Synthesis of (–)-Anisatin. *Org. Lett.* **2012**, *14*, 1632–1635.
- (26) Bunch, L.; Krogsgaard-Larsen, P.; Madsen, U. Mixed Cyano-Gilman Cuprates-Advances in Conjugate Addition to Alpha, Beta-Unsaturated Pyroglutaminol. *Synthesis* **2002**, *2002*, 31–33.

- (27) Synthesis will be reported elsewhere.
- (28) Hansen, K. B.; Bräuner-Osborne, H.; Egebjerg, J. Pharmacological Characterization of Ligands at Recombinant NMDA Receptor Subtypes by Electrophysiological Recordings and Intracellular Calcium Measurements. *Comb. Chem. High Throughput Screening* **2008**, *11*, 304–315.
- (29) Yung-Chi, C.; Prusoff, W. H. Relationship between the Inhibition Constant (KI) and the Concentration of Inhibitor Which Causes 50 per Cent Inhibition (I50) of an Enzymatic Reaction. *Biochem. Pharmacol.* **1973**, *22*, 3099–3108.
- (30) Hedegaard, M.; Hansen, K. B.; Andersen, K. T.; Bräuner-Osborne, H.; Traynelis, S. F. Molecular Pharmacology of Human NMDA Receptors. *Neurochem. Int.* **2012**, *61*, 601–609.
- (31) Uchida, Y.; Tachikawa, M.; Obuchi, W.; Hoshi, Y.; Tomioka, Y.; Ohtsuki, S.; Terasaki, T. A Study Protocol for Quantitative Targeted Absolute Proteomics (QTAP) by LC–MS/MS: Application for Inter-Strain Differences in Protein Expression Levels of Transporters, Receptors, Claudin-5, and Marker Proteins at the Blood–Brain Barrier in ddY, FVB, an. *Fluids Barriers CNS* **2013**, *10*, 21.
- (32) Rautio, J.; Humphreys, J. E.; Webster, L. O.; Balakrishnan, A.; Keogh, J. P.; Kunta, J. R.; Serabjit-Singh, C. J.; Polli, J. W. In Vitro P-Glycoprotein Inhibition Assays for Assessment of Clinical Drug Interaction Potential of New Drug Candidates: A Recommendation for Probe Substrates. *Drug Metab. Dispos.* **2006**, *34*, 786–792.
- (33) Löscher, W.; Potschka, H. Blood-Brain Barrier Active Efflux Transporters: ATP-Binding Cassette Gene Family. *NeuroRx* **2005**, *2*, 86–98.
- (34) Liu, L.; Cao, Y.; Chen, C.; Zhang, X.; McNabola, A.; Wilkie, D.; Wilhelm, S.; Lynch, M.; Carter, C. Sorafenib Blocks the RAF/MEK/ERK Pathway, Inhibits Tumor Angiogenesis, and Induces Tumor Cell Apoptosis in Hepatocellular Carcinoma Model PLC/PRF/5. *Cancer Res.* **2006**, *66*, 11851–11858.
- (35) Si, C.; Myers, A. G. A Versatile Synthesis of Substituted Isoquinolines. *Angew. Chem., Int. Ed.* **2011**, *50*, 10409–10413.
- (36) Akazawa, T.; Uchida, Y.; Tachikawa, M.; Ohtsuki, S.; Terasaki, T. Quantitative Targeted Absolute Proteomics of Transporters and Pharmacoproteomics-Based Reconstruction of P-Glycoprotein Function in Mouse Small Intestine. *Mol. Pharmaceutics* **2016**, *13*, 2443–2456.
- (37) Gynther, M.; Pickering, D. S.; Spicer, J. A.; Denny, W. A.; Huttunen, K. M. Systemic and Brain Pharmacokinetics of Perforin Inhibitor Prodrugs. *Mol. Pharmaceutics* **2016**, *13*, 2484–2491.
- (38) Hansen, K. B.; Ogden, K. K.; Yuan, H.; Traynelis, S. F. Distinct Functional and Pharmacological Properties of Triheteromeric GluN1/GluN2A/GluN2B NMDA Receptors. *Neuron* **2014**, *81*, 1084–1096.
- (39) Hansen, K. B.; Tajima, N.; Risgaard, R.; Perszyk, R. E.; Jørgensen, L.; Vance, K. M.; Ogden, K. K.; Clausen, R. P.; Furukawa, H.; Traynelis, S. F. Structural Determinants of Agonist Efficacy at the Glutamate Binding Site of N-Methyl-D-Aspartate Receptors. *Mol. Pharmacol.* **2013**, *84*, 114–127.
- (40) Assaf, Z.; Larsen, A. P.; Venskutonytė, R.; Han, L.; Abrahamsen, B.; Nielsen, B.; Gajhede, M.; Kastrup, J. S.; Jensen, A. a.; Pickering, D. S.; Frydenvang, K.; Gefflaut, T.; Bunch, L. Chemoenzymatic Synthesis of New 2,4-Syn-Functionalized (S)-Glutamate Analogues and Structure-Activity Relationship Studies at Ionotropic Glutamate Receptors and Excitatory Amino Acid Transporters. *J. Med. Chem.* **2013**, *56*, 1614–1628.
- (41) Sagot, E.; Pickering, D. S.; Pu, X.; Umberti, M.; Stensbøl, T. B.; Nielsen, B.; Chapelet, M.; Bolte, J.; Gefflaut, T.; Bunch, L. Chemoenzymatic Synthesis of a Series of 2,4-Syn-Functionalized (S)-Glutamate Analogues: New Insight into the Structure-Activity Relation of Ionotropic Glutamate Receptor Subtypes 5, 6, and 7. *J. Med. Chem.* **2008**, *51*, 4093–4103.
- (42) Alcaide, A.; Marconi, L.; Marek, A.; Haym, I.; Nielsen, B.; Møllerud, S.; Jensen, M.; Conti, P.; Pickering, D. S.; Bunch, L. Synthesis and Pharmacological Characterization of the Selective GluK1 Radioligand (S)-2-Amino-3-(6-[³H]-2,4-Dioxo-3,4-dihydrothieno[3,2-D]pyrimidin-1(2H)-Yl)propanoic Acid ([³H]-NF608). *MedChemComm* **2016**, *7*, 2136–2144.